O'Brien Gary (Orcid ID: 0000-0002-0859-7986)

Wheaton Joseph (Orcid ID: 0000-0002-8361-8150)

Fryirs Kirstie (Orcid ID: 0000-0003-0541-3384)

Mapping Valley Bottom Confinement at the Network Scale

Running Title: Mapping Valley Bottom Confinement

Gary R. O'Brien[1]

Joseph M. Wheaton[1]

Kirstie Fryirs[2]

William W. Macfarlane[1]

Gary Brierley[3]

Kelly Whitehead[4]

Jordan Gilbert[1]

Carol Volk[4]

This article has been accepted for publication and undergone full peer review but has not been through the copyediting, typesetting, pagination and proofreading process which may lead to differences between this version and the Version of Record. Please cite this article as doi: 10.1002/esp.4615

[1]Department of Watershed Sciences, Utah State University, Logan, UT 84322-5210

[2]Department of Environmental Sciences, Macquarie University, North Ryde, NSW, 2109, Australia

[3]School of Environment, University of Auckland, Auckland, New Zealand

[4]South Fork Research, Inc, North Bend, WA 98045

Corresponding author: Gary R. O'Brien: gary.obrien@usu.edu

For Submission to Earth Surface Processes and Landforms as Research Article and follow up to ESEX article by Fryirs*, et al.* (2016):

- 2016. Fryirs K, Wheaton JM, and Brierley G. An approach for measuring confinement and assessing the influence of valley setting on river forms and processes. Earth Surface Processes & Landforms. DOI: 10.1002/esp.3893

Key words: confinement, rivers, drainage network, River Styles, fluvial geomorphology, river restoration

Abstract

In this paper, we demonstrate the application of a continuous confinement metric across entire river networks. Confinement is a useful metric for characterizing and discriminating valley setting. At the reach scale, valley bottom confinement is measured and quantified as the ratio of the length of channel confined on either bank by a confining margin divided by the reach length. The valley bottom is occupied by the contemporary floodplain and/or its channel(s); confining margins can be any landform or feature that makes up the valley bottom margin, such as bedrock hillslopes, terraces, fans, or anthropogenic features such as stopbanks or constructed levees. To test the reliability of calculating confinement across entire networks, we applied our geoprocessing scripts across four physiographically distinct watersheds of the Pacific Northwest, USA using freely available national datasets. Comparison of manually digitized and mapped with modelled calculations of confinement revealed that roughly 1/3 of reaches were equivalent and about 2/3 of the sites differ by less than ±15%. A sensitivity analysis found that a 500 m reach segmentation length produced reasonable agreement with manual, categorical, expert-derived analysis of confinement. Confinement accuracy can be improved (circa 4% to 17% gains) using a more accurately mapped valley bottom and channel position (i.e., with higher-resolution model inputs). This is particularly important when differentiating rivers in the partly confined valley setting. However, at the watershed scale, patterns derived from mapping confinement are not fundamentally different, making this a reasonably accurate and rapid technique for analysis and measurement of confinement across broad spatial extents.

Introduction

Understanding how and why a river channel adjusts on a valley bottom is a key component of river science and management. Geomorphologists have developed a good understanding of primary controls upon channel geometry and planform in fully alluvial settings in which the channel creates its own morphology, based upon relations between slope, discharge, bed material size and bank strength (e.g., Eaton and Millar, 2017). Such situations contrast starkly with fully imposed (forced) morphologies of bedrock rivers (e.g., Tinkler and Wohl, 1998). Differentiation of bedrock and alluvial rivers define end-member conditions along the spectrum of geomorphic river diversity. These end-members, and the continuum of rivers that lie between them, are influenced by confinement, which characterizes the extent to which a channel freely adjusts across a the valley bottom (Fryirs and Brierley, 2010; Fryirs*, et al.*, 2016). This paper develops and tests a geoprocessing procedure that determines the spatial variability of reach-scale confinement across drainage networks.

Geomorphologists have long used absolute measures of channel width and valley width to analyze the scale and scope for channel adjustment on the valley bottom (Montgomery and Buffington, 1998; Rosgen, 1994; Wolman and Miller, 1960). Traditionally, the ratio of channel width to valley width has been used as a normalized index for discriminating process regimes in different valley settings (cf. Alber and Piegay, 2011; Hall*, et al.*, 2007). Nagel*, et al.* (2014) employed network and DEM inputs to calculate confinement based on cost-weighted distance (sensitivity or “cost” to changing slope values with lateral distance in raster analysis), flood height, slope and maximum valley width. However, such measures produce

only confined and unconfined binaries that occur on either side of a discrete valley width:bankfull width threshold (Wohl, 2013; Wohl*, et al.*, 2012). Similar measures, such as entrenchment ratios (e.g., Rosgen, 1996), use the ratio of bankfull channel width to width at 2x bankfull height. Similarly, Roux*, et al.* (2015) and Gilbert*, et al.* (2016) developed a suite of GIS-based tools designed to extract valley bottoms for use in measuring valley confinement. All these approaches rely on accurate quantification of the width dimension of features on the valley bottom.

However, as Figure 1A illustrates, a simple ratio of valley bottom (or valley) width to bankfull width can fail to discriminate some fundamentally different geomorphic settings. This is not to suggest absolute measures of channel and valley bottom width are not useful. Part of their utility rests in the simplicity with which they can be calculated and their conceptual elegance. However, such approaches do not take into account the position of the channel on the valley bottom or the extent of confining margins encountered by an active channel. This is a distinct and important characteristic of the confinement approach proposed by Fryirs*, et al.* (2016), aiding differentiation of valley settings along a river course. Moreover, this method poses a significant advantage over existing tools because outputs can be linked directly to interpretations of the capacity for channel adjustment (e.g., they illustrate baseline boundary conditions imposed on the channel by the valley and valley landforms) and by extension, to analyses of river channel sensitivity.

In Fryirs*, et al.* (2016) we proposed that a measure of 'confinement' based on length ratios is equally simple to measure, but less sensitive to the precision of width measurements or underlying mapping, and is a better discriminator of valley settings.

In Fryirs*, et al.* (2016), we defined confinement as the percentage of length of a channel margin that abuts a confining margin on either bank. Building on a taxonomy proposed by Wheaton*, et al.* (2015) that defined margin types for geomorphic features on the valley bottom, Fryirs*, et al.* (2016) laid out consistent definitions for calculating three types of confinement: valley confinement, valley bottom confinement and anthropogenic confinement (Figure 1B).

Quantification of confinement provides a basis to differentiate between confined, partly confined and laterally unconfined valley settings (Brierley and Fryirs, 2005; Fryirs*, et al.*, 2016) whereby the degree to which river morphology reflects an imposed condition varies along a confinement continuum from no contact (i.e. 0%) to continuous contact (i.e.100%) of the channel with a confining margin. Brierley and Fryirs (2005, see §9.3.1.1) cautiously suggested approximate confinement value breaks of 10% for the transition between laterally unconfined and partly confined; and 90% for the transition between partly confined and confined. Physically, this differentiation of confined, partly confined and laterally unconfined valley settings reflects whether floodplains are continuous, discontinuous, occasional or absent altogether, respectively (Figure 2).

The emergence of high resolution topography (HRT) now supports production of digital elevation models (DEMs) with 2 m resolution and higher that can be used for a range of different geomorphic applications, including analysis of confinement (Passalacqua*, et al.*, 2015; Stout and Belmont, 2013). While coverage of HRT is ever growing (with nationwide coverages emerging in some smaller nations), the reality in most locations on earth (including most of the US) is that HRT is on the horizon as

opposed to being readily available today. Moreover, even if HRT were ubiquitous and available now, from a pragmatic perspective we face non trivial computational challenges when such datasets are applied at broad spatial scales (Schaffrath*, et al.*, 2015) or across entire drainage networks with sizeable watershed area (i.e. > 100 km^2). However, this should not halt the process of using available datasets to achieve the same outcome. For example, there are far more watersheds across the world for which intermediate resolution topography datasets (hereafter "coarse-resolution inputs") datasets are available (e.g. Table 1). This presents an opportunity for wide-ranging, comparative geomorphic assessment across different settings, thereby supporting, for example, region-wide analyses of river diversity (e.g., Bizzi*, et al.*, 2018; Demarchi*, et al.*, 2016)

This paper presents a pragmatic geoprocessing approach for measuring confinement and uses it to explore how well valley bottom confinement can be measured and mapped using coarse-resolution inputs such as 5 to 10 m resolution digital elevation models (DEMs; e.g. National Elevation Datasets - NED in USA; (USGS, 1999)), and nationally available stream networks (e.g. National Hydrography Dataset – NHD (McKay*, et al.*, 2012)). We then test how well the GIS algorithm outlined below can be applied across entire drainage networks to continuously map and discriminate valley settings. Our working hypothesis is that coarse-resolution inputs will be adequate to differentiate the most fundamental differences in valley settings. A sensitivity analysis verifies the differentiation of valley setting output across four watersheds in the Columbia River Basin in the US Pacific Northwest.

Methods

Confinement Calculation Workflow

The calculation of the three forms of confinement outlined in Fryirs*, et al.* (2016) (valley confinement, valley bottom confinement and anthropogenic confinement) take the form of:

Equation 1 $$C = ((\sum_{DS}^{US} CL_{EB}@CM)/CL_T) \times 100$$

where C is confinement (between 0 and 100%), $\sum_{DS}^{US} CL_{EB}$is the sum total centerline length of channel over the distance that the channel margin along either bank abuts a confining margin (@*CM*), and CL_T is the total centerline length of a channel segment under consideration. It is important to note that the measure of $CL_{EB}@CM$does not double-count where the channel is confined along both banks and overlaps, which is a measure of *constriction*; see Fryirs*, et al.* (2016). Also note that we use the term *segment* as a noun to describe the portion of the network polyline being analyzed, and not as a proxy for a river reach defined by geomorphic characteristics and a distinctive structure and function such that a relatively uniform morphology results (Fausch*, et al.*, 2002; Kellerhals*, et al.*, 1976).

Confinement is a dimensionless quantity, but its value is sensitive to the segment length (CL_T) over which it is calculated. The input quantities $\sum_{DS}^{US} CL_{EB}@CM$ and CL_T are straightforward to measure manually off maps or imagery of sufficient resolution and detail, or in the field for a single river reach (Figure 3). Below, we describe a geoprocessing workflow with which the confinement value can be calculated and

attributed to every segment across an entire drainage network and applied continuously at the network scale. The primary inputs from which calculations are derived are two polygon inputs, one representing the bankfull channel margin boundaries, and the other representing the potential confining margins (i.e. valley margin, valley bottom margin, or anthropogenic margin). It is important to note that currently, our method provides a single confinement output (continuous values from 0.0 to 1.0) and does not automatically classify valley confinement (C_V), valley bottom confinement (C_{VB}), and anthropogenic confinement (C_A) separately. To differentiate these confinements as outputs, a user needs to consciously run the tool each time with potential confining margins representing valley margins, valley bottom margins and/or anthropogenic margins separately.

Manual implementation of the confinement calculation workflow is straightforward, but for ease of application over large drainage networks we developed a geoprocessing toolbox for ArcGIS. We refer to this GIS algorithm as the Confinement Tool (see:http://confinement.riverscapes.xyz). The source code is freely available (https://github.com/Riverscapes/ConfinementTool) and written in Python with ArcPy libraries. The 'tool' has not yet been refactored into an easy-to-use, stand-alone or Add-In without Arc version-specific dependencies, and sophisticated error handling. As such, the open-source tool should allow experienced GIS users, with some Python proficiency to reproduce the results presented here or apply the model with similar data in their areas. Moreover, experienced programmers can extend the code for their own applications or refactor it altogether. However, it would be an over-statement to imply this tool is ready to apply anywhere. That said, the methods are simple, robust and easily extendible to any part of the world where the inputs can be produced.

Network Preparation and Processing Extent

A polyline drainage network is needed as a primary model input as it represents the centerline position of the active channel, and provides the basis to define reaches. From this we can specify the reach length over which confinement is calculated and resolved. Acquiring or deriving the drainage network is the first step in the confinement calculation process (Figure 3, Step 1). If deriving a network from scratch, this can be done manually (i.e. digitizing from imagery), or automatically from digital elevation models (DEMs) through flow accumulation based algorithms (Holmgren, 1994; Lindsay, 2016). Alternatively, in many countries, regions and municipalities, existing base hydrography and/or drainage network layers exist (e.g. NHD in the USA and National Surface Hydrology Database in Australia (Table 1). If using existing hydrographic networks, we recommend using cartographically derived (i.e. manually digitized) products (e.g. NHD 1:24K as opposed to NHD+ 1:100K in the USA) over hydrographically derived networks produced from coarse-resolution DEMs (e.g. >5m resolution). While LiDAR derived drainage networks may be used (e.g., Passalacqua*, et al.*, 2015), some caution should be exercised as these may include too many fine-scale watercourses (e.g. ditches, swales, curbs and gutters), thereby increasing the processing time and hindering interpretation of the output.

An optional step in network preparation is to subset the drainage network to the desired processing extent (e.g. the drainage basin of interest, or part(s) thereof). In some applications, it may be desirable to filter out ephemeral and intermittent watercourses and only focus on perennial watercourses. Similarly, many digital drainage networks have anthropogenic ditches and canals, whereas some have

‘artificial connectors’ (e.g., across a reservoir or a swamp) to maintain topological and hydrologic connectivity. If the positional accuracy of the drainage network is inadequate, manual editing of the network geometry may be warranted to achieve better alignment with actual channel position (e.g. using underlying base imagery or mapping).

Finally, the network can be segmented as appropriate to the application (Figure 3, Step 2). This will determine the CL_T length over which confinement is calculated. If CL_T is too short, the confinement calculation will overestimate both high and low values (i.e. producing confined and laterally unconfined results), while underestimating partly confined situations (i.e. intermediate confinement). If CL_T is too long, it may mute out important occurrences of shorter confined or laterally unconfined segments. Various coordinate geometry (COGO) and geoprocessing algorithms exist for uniformly segmenting the network. Examples include designation of junctions using uniform segment lengths (e.g. every 500 m or 1000 m; e.g., http://gnat.riverscapes.xyz/). Some algorithms can apply a variable segmentation length (e.g. as a function of stream order or drainage area; (Roux*, et al.*, 2015; Williams*, et al.*, 2013)). It may be desirable to add additional segment breaks where the drainage network is intersected by lithological or landscape unit boundaries.

Generate Channel and Confining Margin Polygons, and Derive Zone of Confinement Intersection

As illustrated in Figure 3, Step 3, a channel margin polygon is needed to approximate the edge of the active channel. In some situations, this may be analogous or even equivalent to a bankfull polygon. This is generally, but not always,

outside a low-flow or base-flow wetted edge margin. Channel margins could be automatically derived from high-resolution DEMs, hydraulic model simulations, image classification, field mapping, or manual digitizing of channel margins from aerial photography or high resolution DEMs. Alternatively, a channel margin could be approximated by applying a buffer (representing the active channel width) to a drainage network centerline. Simple regressions of active channel width to drainage area (e.g. Beechie and Imaki, 2014) may suffice as an approximation. In this study, we refer to the "active channel" as a bankfull polygon derived from a width offset to the input network centerline, as a function of drainage area (e.g., regional curve for bankfull width). Channel margins derived from higher resolution sources are more precise and have a higher positional accuracy than cruder approximations like network buffers. However, across large drainage networks, a simple network buffer may suffice for deriving confinement values and effectively discriminating among valley settings.

Depending on the type of confinement that is being calculated (i.e. valley, valley bottom or anthropogenic), a polygon layer of that potential confining margin is needed (Figure 3, Step 1). As with the other inputs, this can be automatically derived from DEMs, or it may be manually derived either in the field or from existing layers using a combination of topographic and aerial photographic evidence. If the potential confining margin is anthropogenic, mapping of features like levees, roads, and railroads may be used. If the potential confining margin is a valley margin, geomorphic mapping of the valley bottom features (i.e. active channel and floodplain) need to be differentiated from bedrock hillslope features, fans and terraces to define the valley margin (O'Brien*, et al.*, 2019; Stout and Belmont, 2014).

If the potential confining margin is a valley bottom margin, a variety of methods exists for deriving the valley bottom including 1.5D, 2D or 3D hydraulic modeling, manual delineation, the Fluvial Corridor Tool (Roux*, et al.*, 2014) or the VBET – Valley Bottom Extraction Tool (Gilbert*, et al.*, 2016). Depending on the resolution and scale of the valley bottom polygon being used, it may be necessary to provide a small buffer (similar to resolution of mapping) on the channel extent to ensure an intersection. For experiments reported in this paper, we used valley bottoms derived from a 10 m NED DEM and manually edited (for occasional resolution errors occurring at the margin between hillslope and valley bottom; cf. Gilbert*, et al.* (2016). These polygons comprise the valley bottom margin and do not differentiate valley margin, valley bottom margin, or anthropogenic confinement.

The confining margin (pink segments of potential confining margin in Figure 3, Step 5) is the portion of the potential confining margin that actually abuts the active channel. A simple intersection approach can be used to derive the confining margin using geoprocessing procedures. A buffer on the channel margin is needed to make an intersection between an abutting or immediately adjacent channel margin and the potential confining margin (Figure 3, Step 4). Depending on the resolution of base mapping from which the channel margin and potential confining margin are derived, different buffer widths may be appropriate. In general, an appropriate buffer is roughly 1.5 to 2 times the resolution or horizontal precision of the DEM.

Confinement Calculation

To calculate confinement using Equation 1, CL_T and $\sum_{DS}^{US} CL_{EB}@CM$ are needed for each segment. As illustrated in Figure 3, Step 2, CL_T is measured along the channel

centerline from the start of the segment to the end of the segment. It is important that $\sum_{DS}^{US} CL_{EB}@CM$ is also summed and calculated along the centerline, as opposed to measuring the length of the confining margin polyline segments, which could skew the percentages to be longer on outside bends or shorter on inside bends. As shown in Figure 3, Step 6, the measurement along the centerline is made by deriving perpendicular lines from the confining margin end points and intersecting them with the centerline. These perpendicular lines effectively break the reach of interest into a series of smaller segments, each of which have their lengths calculated. Moving along every segment, the $CL_{EB}@CM$ is measured and counted if it corresponds to a zone of confinement on either bank (Figure 3, Steps 6 and 7).

Model output is a continuous quantification of confinement where every reach segment has a value between 0-100%. This can then subsequently be categorized for cartographic or interpretive purposes. In this paper we present our confinement results and analyses using the valley setting classification presented in Fryirs*, et al.* (2016) reproduced here in Table 2 and shown in Figure 2). We separately designate the continuous valley bottom confinement output values in terms of categorical breaks (the primary categories being laterally unconfined, partly confined, and confined, using percent valley bottom confinement breaks of 10% between laterally unconfined and partly confined, and a break of 90% between partly confined and confined). We further differentiated the partly confined valley setting into margin-controlled (specific cases of which may be bedrock margin-controlled, or terrace margin-controlled) and planform-controlled (cases where the channel and floodplain is self-adjusting between intervals of contact with confining margins) (cf. Fryirs and Brierley, 2010).

Case Study Watershed Applications

To illustrate the utility and validity of the above workflow, we applied the confinement algorithm using a 10m DEM (see Gilbert*, et al.*, 2016; USGS, 2007) along streamlines of four watersheds in the Columbia River Basin in the US Pacific Northwest. (Figure 4; Table 3). These basins were chosen because they span a wide range of landscapes, ecoregions, relief and lithologies (Omernik and Griffith, 2014; Thorson*, et al.*, 2003). Channel margins were derived by buffering the perennial portion of the NHD 1:24,000 cartographic drainage network using an empirical regression for bankfull width to drainage area developed by Beechie and Imaki (2014) for the Columbia River Basin. Derivation of drainage area to drive the conversion was obtained from a flow accumulation calculation.

Verification and Sensitivity to Segment Length Analysis

We used three methods to assess sensitivity to the segment length of individual segments comprising the drainage network. An optimized segment length was used in separate exercises to validate model runs using the Confinement Tool.

As indicated earlier, the segment length (CL_T) is one of the most important choices in preparing model inputs. To explore the sensitivity to confinement values to CL_T length quantitatively and robustly, we segmented the input drainage network of the Upper Salmon watershed at 250, 500, 750, 1000, 1500, 2000, 2500, 3000, 4000 and 5000 m segment lengths. In Figure 5 we show how different maximum segmentation lengths result in different confinement outputs. Segment lengths should not be less than the channel width or the typical length scale of geomorphic units (i.e. > 1-3

channel widths), but should not be so long as to miss important geomorphic breaks (i.e. they should typically be < 5 km).

We compare these calculations with an entirely expert-derived, manually classified confinement, which does not rely on segmentation but rather on visible geomorphic attributes to locate reach breaks. This *"expert manual confinement"* or EMC was performed following the method of Brierley and Fryirs (2005, see §9.3.1.1). EMC refers to a method of visually determining diagnostic geomorphic features comprising individual reach types, then using that information to delineate the valley setting and underlying confinement for an entire stream network. This produces "manually derived, categorical results" For this study, we used imagery to map reach breaks (boundaries between adjacent reaches), and (a) channel planform; (b) presence/absence and extent of floodplains; (c) confining margin and constriction proportion (see Fryirs*, et al.*, 2016); (d) generalized instream geomorphic units and bed material caliber. In the case of the Upper Salmon watershed, we verified our manual delineation of reach types and valley setting with more than 30 field checks of our remotely sensed assessments. We transferred the km-scale information to the network in a GIS editing session (see O'Brien and Wheaton (2015); O'Brien*, et al.* (2017)).

Overall Accuracy of Using the Confinement Tool Compared to Expert Manual Confinement (EMC)

We performed two types of verification to evaluate the workflow that drives the Confinement Tool. Both were done using trial runs in the Upper Salmon watershed. The first form of verification was to compare the model-calculated values of

confinement to manually delineated valley settings using EMC. For this analysis, we derived from the distribution of confinement values the percent of stream kilometers in each of these bins determined by categorical breaks as well as exploring other breakpoints. For example, we tested the break between partly confined and confined valley settings that were presented in Brierley and Fryirs (2005) as occurring at 90%. We tested whether a break point at 85% may better reflect confined rivers to account for those rivers that have occasional floodplain pockets (e.g. at tributary confluences or local valley widening) but their morphology is dominated by confinement. In addition, we compared predicted categorical calls on every polyline segment for 729 km of streams and 2092 individual segments. We used multiple segment lengths to evaluate sensitivity and used these results to choose the most appropriate segment length to run the Confinement Tool across the basin.

As a separate form of verification, we directly compared model outputs to manually *measured and calculated* values of confinement from the Upper Salmon watershed (Figure 6). This process is the same as EMC described above, but with additional steps to increase the accuracy of the calculated confinement. To do this, we took a random sample of 50 confined, 100 partly confined (parsed as 50 planform-controlled and 50 margin-controlled) and 50 laterally unconfined polyline segments using the *r.sample* command in GME (Geospatial Modeling Environment; Spatialecology.com). In each segment, we used the same CL_T inherited from the segmented NHD network, but independently assessed the valley bottom margin along each randomly selected segment with air photos and independently calculated valley bottom confinement using digitized stream lengths and digitized confining margins. Residuals were compared to assess overall performance of the model

when run with coarse-resolution inputs (i.e., the NHD streamlines; inset photos of Figure 6). We hypothesized that using hand-digitized stream lengths and confining margins would produce a more accurate snapshot of the actual confinement than the modeled output resulting from coarse-resolution inputs. To test this, we plotted confinement against total stream length in three ways: (a) as output from the Confinement Tool using the NHD streamline; (b) output from the Confinement Tool using *manually digitized stream lengths* as the streamline input; and (c) manually digitized and measured stream lengths and confining margins (EMC), calculated using equation 1, entirely independently from the Confinement Tool. The two model runs (items a and b, above) used buffered bank full polygons derived from their NHD and manually digitized streamlines, respectively, but employed the same valley bottom polygon.

Influence of Input Map Layer Resolution and Quality

Although the primary purpose of this paper is to explore how well valley bottom confinement can be calculated across entire drainage networks using coarse-resolution inputs, we were particularly interested in whether or not the model was getting the 'wrong answer for the right reasons'. In other words, we would be satisfied with the validity of the confinement algorithm if the places it diverges from a manually derived calculation is based on having poor inputs such as an inaccurate valley bottom delineation, or a poor quality stream network that misplaces the position/location of the channel on the valley bottom. It is logical that higher resolution inputs and more precise mapping of potential confining margins and channel margins will yield more accurate results. To test this assertion, we compared model outputs using nationally available inputs from the Tucannon watershed with a

valley bottom polygon derived from a 1 m DEM, using VBET (cf. Gilbert*, et al.*, 2016), and with a channel margin that was manually digitized from LiDAR data and concurrent high resolution aerial imagery obtained from Watershed Sciences (2010).

Results and Interpretation

Verification and Sensitivity to Segment Length Analysis

The primary verification output we used was from the Upper Salmon watershed, Idaho. Figure 7B shows an example of the Confinement Tool output using the original unedited geometry of the NHD drainage network segmented with a maximum segmentation length of 500 m and based on a valley bottom derived from a 10 m NED DEM and manually edited. Figure 7B is based on a continuous quantification of confinement (i.e. every reach segment has a value between 0 and 100%), but has been symbolized using categorical breaks for different confinement classes described above.

Qualitatively, the map compares very favorably with the independently derived EMC shown in Figure 7A. Both results (Confinement Tool output and EMC) were conducted on the same segmented NHD network. The largest discrepancies occur in the higher order streams (Table 4) where there is a tendency for the Confinement Tool to split out smaller segments into confinement settings that differ from their neighbors. Often, whereas the manual delineation using EMC lumps longer consecutive segments of the same confinement category.

To illustrate the sensitivity of the Confinement Tool output C compared with manually derived, categorical results (EMC) we plotted a succession of segment lengths relative to the total network stream length in the Upper Salmon watershed (Figure 8). The resulting plots show that estimates derived using longer segment lengths tend to underestimate laterally unconfined settings and overestimate the portion of confined and partly confined, margin-controlled settings. The process of segmenting the native NHD drainage network produces a large percentage of segments that are shorter than the target segment length. This is most pronounced with longer segment lengths (e.g. 5000 m), and least with short segment lengths (250-500 m) because a greater number of low order tributaries and shorter segments forced by network topology are omitted with increased segment length. Figure 8B shows the confinement data plotted against total stream length using only segment lengths that are exactly as indicated (e.g. 250, 500, etc.). Viewed another way, Figure 8C is the frequency of network segments within percent confinement categories segmented at multiple lengths. Comparison of EMC and modeled confinement suggests that laterally unconfined reaches are somewhat under predicted (but best represented by shorter segment runs), whereas partly confined and confined settings are best represented by model outputs using the network segmented at 500 m. The results of these two outputs (EMC and 500 m segment model output) at the watershed scale are shown in Figure 7.

Figure 9 shows the results of a test of the average segment length inherent in the base cartographically derived NHD drainage networks for the Tucannon, Grande Ronde, Middle Fork John Day, and Upper Salmon watershed. All were clipped to the perennial extent. The average segment length of 466 m is similar to the best fit result

we found in the Upper Salmon of 500 m. Based on topology of the NHD networks, this suggests that 500 m segments are most suitable for calculating confinement when compared to the average segment lengths representing confluence to confluence characteristics of these watersheds.

Overall Accuracy Compared to Manual Delineations

To gauge the accuracy of modeled output, we compared results of modeled and EMC in the Upper Salmon watershed (see Figure 7). Confinement determined by EMC has limited precision because channel planform and confining margins are visually assessed and not digitized and measured; yet, it is arguably an accurate technique for assessing the geomorphic setting because we rely on rigorous air photo reconnaissance and field checks (e.g., O'Brien*, et al.* (2017), Plate 3) to identify diagnostic features of the valley, channel and floodplain. Modeled confinement, on the other hand, is internally precise but is generally inaccurate with respect to actual landscape contours. This arises because the valley bottom and buffered bankfull produced from a 10 m DEM and the coarse nature of NHD network fail to capture subtleties (and oftentimes, large scale) features of the geomorphic setting (see Figure 6, inset photos A and B).

We compared the distribution of categorical EMC versus modeled confinement for the Upper Salmon watershed (n = 2089 network segments; Figure 10) to quantify the level of agreement. Although the interquartile range exceeds the estimated categorical breaks of each category (laterally unconfined <10%; partly confined 10-50% and 50-85%; and confined >85%), the median values are well within each category, and reasonably close to their central values. Importantly, modeled

confinement values differ significantly between each manual classification. Our modelled results suggest that a better breakpoint at 85% occurs to reflect the confinement transition from partly confined to confined valley settings. As this is empirical, this may be interesting to explore how well these categorical breaks hold in other physiographic settings.

Several insights emerged from our study of 207 randomly selected and analyzed reaches shown in Figure 6. Quantitatively, the model output displayed ~10% more confined reaches, significantly more laterally unconfined reaches, and correspondingly fewer numbers of partly confined reaches, than did confinement calculated using EMC (e.g., manually digitized streamlines *and* confining margins calculated using Equation 1). When digitized streamlines were used in place of the NHD drainage network as the model input, results were similar to those calculated manually, but with proportionally more partly confined and fewer confined streams (Figure 11). In this case, we recognize that coupling cartographically realistic, hand-digitized planform segments with valley bottoms and bankfull channel polygons derived from low-resolution base layers may not increase the realism and accuracy of confinement calculations (see later).

To further compare the model outputs versus EMC and modeled results for the randomly selected streamline dataset, we produced a distribution of difference and regression. Figure 12 shows that 30% of all confinement values are equivalent, and about half (45%) differ only ±5% (n = 207). Moreover, 67% of the sites differ by less than ±15%. Most of the agreement in this comparison rests with end member confinement values equal to 0 and 1 (i.e., where the valley setting is clearly confined

or laterally unconfined). This is because the modeled output (using coarse-resolution inputs) versus EMC are less likely to diverge when the valley setting is clearly laterally unconfined or confined. However, the opposite is true of partly confined, margin-controlled and partly confined, planform-controlled settings, where manually digitized streamline and confining margins are likely to produce more precise calculation of partly confined reaches than would a model output using coarse input products. Despite the difference between inputs for this analysis, the relationship between the manually digitized EMC versus modeled has an $r^2 = 0.64$ and nearly half vary only slightly.

Influence of Input Map Layer Resolution and Quality

Higher resolution input datasets might produce more precise measures of reach-scale confinement across networks. To illustrate this, we compared valley bottom and bankfull polygons using 1 m and 10 m base DEMs, and streamlines derived from their respective rasters for the mainstem Tucannon River (Figure 13 and Table 5). Using a 1 m DEM resulted in significantly greater total stream length relative to a 10 m DEM (156 km versus 118 km, owing to increased planform sinuosity detectable by LiDAR and anabranching channels in some places). In terms of confinement, the amount of laterally unconfined reaches was nearly double that produced by a 10 m DEM, whereas the proportion of partly confined and confined reaches was reduced.

High-resolution vector and raster data inputs (e.g., 1 m DEM with digitized stream lines) produces the clearest, most realistic results, with greater certainty than when using lower resolution inputs. In these watersheds, modeled confinement from

nationally available datasets appears to underestimate laterally unconfined valley settings to a greater degree than confined valley settings.

Discussion

Significance and current limitations

Our analysis of valley bottom confinement across entire drainage networks provides a coherent, relatively rapid assessment of valley setting. This is not the first large-extent assessment of valley setting presented at a network scale (e.g., Nagel*, et al.*, 2014; Roux*, et al.*, 2015), but it is the first to use and validate the discriminating definitions of confinement that account for channel position on the valley floor and quantify lengths of channel margin that are in contact with confining margins. Previous attempts to quantify valley setting have emphasized the ratio of channel width to valley bottom width (e.g. Beechie and Imaki, 2014; Benda*, et al.*, 2007). While such a ratio is useful in as far as it is dimensionless, we nevertheless see two important limitations.

First, reliable and accurate measurements of channel width are not widely available and deriving them from remote sensing data requires high-resolution topography (e.g. LiDAR) or imagery without strong interference from vegetation (Notebaert and Piegay, 2013). Valley width is generally easier to derive than channel width across entire drainage networks, but it too is difficult to derive accurately. Even when applied with high-resolution datasets, accuracy of the width measurements remains an issue (Notebaert and Piegay, 2013). The calculation of a valley confinement proxy based on channel width to valley width ratio is therefore very sensitive to the accuracy of those measurements. While the method presented here relies on similar

input datasets (valley bottom and channel polygons, and network datasets), calculations are based on the length of the active channel margin that is confined, rather than channel width, making them less sensitive to the quality of mapping. Also, using spatial averaging eliminates problems with the imprecisions of polygon mapping of channels and valley bottoms. As shown here, modest improvements in accuracy can be achieved with more precise manual mapping of channel and valley margins.

Second, and more fundamentally, width ratios can be misleading as they do not account for the influence of a confining margin on the behavior and lateral adjustment potential of a channel on its valley bottom. Such ratios fail to consider or discriminate the position of the channel on the valley bottom and its interaction with a confining margin. For example, Figure 1A shows that using Equation 1 to calculate confinement results in a literal measure of the river's imposed condition, whereas the CW:VBW ratio is a probabilistic estimate that confinement is likely to occur. As a result, similar or identical CW:VBW scenarios could apply to (or fail to differentiate) a range of valley settings when analyzed at the reach scale. This is because Equation 1 requires the length of active channel margin contact as an input to calculate confinement, whereas a CW:VBW ratio does not.

As the Confinement Tool relies on length measures, it is inherently sensitive to the segment length (CL_T) over which it is calculated (cf. Church, 1996; Reinfelds*, et al.*, 2004). Our sensitivity to segment length exercise showed that gross over- or underestimation of confinement can be avoided by selecting a segment length that is similar to natural confluence-to-confluence nodes in a given catchment. This held

true in our four case study watersheds, but could potentially yield different results given different stream pattern and drainage density configurations.

As determination of CL_T as outlined in this paper is left to the user, any applications of the Confinement Tool require an explicit statement regarding the scale at which the analysis has been conducted and the resolution of the data used. The analysis presented here applies a uniform CL_T across the entire drainage network. While we conduct a sensitivity analysis to help inform a choice of a constant CL_T, this is not the only way to approach the problem. For example, the user could manually or systematically vary CL_T across the drainage network, perhaps derived as a function of drainage area or stream order. Alternatively, a multi-scalar approach could perform the calculations at each node over a range of possible polyline segment lengths and then combine them to estimate a value, or distribution of values. In a related manner, Notebaert and Piegay (2013) presented a technique for calculating measures of floodplain width and aggregating them over various longitudinal length scales. Similarly, the Roux*, et al.* (2014) Fluvial Corridor Tool relies on what they define as unitary graphic objects (or valley bottom cells), which have a variable length scale that is derived adaptively from network measures calculated over a range of length scales. There is significant scope to adaptively segment a drainage network to a variable CL_T, based on natural breaks in the data.

While our analysis using coarse-resolution inputs to derive valley bottoms and channel margins does not produce perfect results, the 500 m segment length applied here derives results that are 90 ± 5% accurate and came from freely, nationally available data. Moreover, the difference between modeled and EMC rests mostly

with the map resolution and quality of input products, and the effort to combine the two methods. Using digitized streams with 10m derived valley bottom resolution does not appear to improve the accuracy of the results using the modeling approach (Figure 13). While the manually digitized and calculated EMC results are generally more accurate, manual digitizing at the network scale at broad scales could be a prohibitively time-consuming process. Hence, we are significantly encouraged by the tool's performance, even where it gets it 'wrong'. The 'wrong answer for the right reasons' is perfectly acceptable (e.g. the mapped channel position is wrong), particularly when applying the approach across drainage networks. In most cases, the predictions are only falling short in locations where the input data are locally inaccurate on account of coarse input datasets. This most commonly occurs where the channel centerline or valley margin is positioned incorrectly (e.g., Figures 6A and B). This is not a shortcoming of the model, but rather a limitation of the input data (Macfarlane*, et al.*, 2015).This should not deter users from leveraging available, coarse-resolution inputs (e.g. 10m DEMs) as an entry-level analysis for reach-scale river typing across entire drainage networks (Lisenby and Fryirs, 2017). Instead of waiting for technology to provide the answer, fundamental geomorphic insights can already be achieved using data that are already available. Moreover, as HRT becomes more available, it is wise to ensure we have the right conceptual frameworks in place, are measuring the right things, and refining and developing our workflows on datasets that are easy to work with.

Examples of Applications of the Confinement Tool

The Confinement Tool developed in this paper can support automated watershed-wide analyses of valley bottom confinement in a repeatable and consistent manner.

Numerous scientific and management applications emerge from this work. For example, the tool can support regional-scale analyses of controls upon river diversity and morphodynamics (cf., Bizzi*, et al.*, 2018; Demarchi*, et al.*, 2017). Figure 14 demonstrates variability in valley setting across the four watersheds analyzed in this study. Such images not only provide communication aids that draw attention to landscape patterns, they also provide quantitative insights into the make-up of each watershed. This variability can be explained in relation to the geologic and physiographic factors outlined in Table 3. In summary terms, the proportion of confined valley settings (36-48%) is far greater than the proportion of laterally unconfined valley settings (8-17%) in the Middle Fork John Day and Tucannon Watersheds (Figures14B and C) as the underlying basalt induces high relief terrain with a high drainage density. In contrast, the proportion of laterally unconfined valleys (25-33% of all streams) is far higher in the Grande Ronde and Upper Salmon Watersheds (Figures 14A and D), associated with lower-relief terrain and attributes of Quaternary landscape history (outwash plains are prominent in the latter instance). Such analyses also draw attention to the prominence of partly confined valley settings, the proportion of which ranges from 33-55% of all streams. This provides a first-order approximation of the capacity for lateral adjustment of differing sections of river course.

As another example, the Confinement Tool can provide helpful complementary insights into controls upon watershed-scale patterns of rivers, accompanying analysis of slope along the longitudinal profile and downstream changes in stream power (see Figure 15)(Bizzi and Lerner, 2015; Reinfelds*, et al.*, 2004). Historically, such analyses have emphasized variability in total stream power, but increasing

refinement in our analyses of the width of the active valley bottom and channel width will support much more powerful insights into broad-scale patterns of unit stream power. In a related manner, further work is required to analyze forms and patterns of lateral constraints upon channel adjustment. The distribution and type of constraint at 'active channel margins' influences the pattern and rate of sediment and wood from eroding banks, providing insight into local, reach, and watershed-scale controls upon the character and behavior of the river. This would support analyses of controls upon channel constrictions and appraisals of impacts of anthropogenic structures upon river morphodynamics, including artificial levees, embanked road and rail lines and river rehabilitation structures. As presented here, inputs can be manually manipulated to classify C_V, C_{VB}, and C_A separately, but as yet the Confinement Tool has not been fully automated to generate such outputs. Potentially, such analyses could further aid interpretations of fluvial landscapes.

Conclusion

Measuring and mapping valley bottom confinement across entire drainage networks is a critical step toward describing and discriminating valley settings across broad spatial scales. In this follow up research article to the ESEX letter presented by Fryirs*, et al.* (2016), we present an approach for measuring confinement across watersheds using nationally available base map layers of intermediate resolution. Our approach builds on, but diverges from, previous developments (e.g., channel width to valley bottom width ratios) to discriminate valley settings by accounting for channel position on the valley bottom and lengths of channel that interact with

potential confining margins.This method for calculating confinement demonstrates the potential for rapid, consistent, assessment of large areas using coarse-resolution products with a reasonable degree of accuracy. Such assessment provides a basis for a wide range of morphometric analyses and applications in geomorphology.

Acknowledgements

The authors wish to thank two anonymous reviewers for their thoughtful suggestions, insights and comments that substantially improved this manuscript. GO and JW (Utah State University) and CV (South Fork Research, Inc) acknowledge grants from the Bonneville Power Administration to Eco Logical Research (ELR), Inc. (BPA Project number 2003-017) GO and JW also acknowledge subsequent grants from ELR to Utah State University (USU award ID: 100652 and 150737), which supported their involvement on the project. GO thanks the Department of Watershed Sciences at Utah State University who provided financial support beyond the above grants to see this manuscript through to completion. Financial support to KF from the Macquarie University Outside Studies Programme provided travel to Utah State University for sabbatical. KF also acknowledges support from the Australian Research Council. GB gratefully acknowledges support from the University of Auckland study leave programme that assisted his work at Utah State University.

References

Alber A, Piegay H. 2011. Spatial disaggregation and aggregation procedures for characterizing fluvial features at the network-scale: Application to the Rhone basin (France). Geomorphology **125**: 343-360. DOI: 10.1016/j.geomorph.2010.09.009

Beechie T, Imaki H. 2014. Predicting natural channel patterns based on landscape and geomorphic controls in the Columbia River basin, USA. Water Resources Research **50**: 39-57. DOI: 10.1002/2013WR013629

Benda L, Miller D, Andras K, Bigelow P, Reeves G, Michael D. 2007. NetMap: A New Tool in Support of Watershed Science and Resource Management. Forest Science **53**: 206-219

Bizzi S, Lerner DN. 2015. The Use of Stream Power as an Indicator of Channel Sensitivity to Erosion and Deposition Processes. River Research and Applications **31**: 16-27. DOI: 10.1002/rra.2717

Bizzi S, Piégay H, Demarchi L, Van de Bund W, Weissteiner CJ, Gob F. 2018. LiDAR-based fluvial remote sensing to assess 50–100-year human-driven channel changes at a regional level: The case of the Piedmont Region, Italy. Earth Surface Processes and Landforms **0**. DOI: doi:10.1002/esp.4509

Brierley G, Fryirs K. 2005. Geomorphology and River Management: Applications of the River Styles Framework. Blackwell Publishing: Victoria, Australia

Church M. 1996. Space, Time and the Mountain - How Do We Order What We See? In *The Scientific Nature of Geomorphology: Proceedings of the 27th Binghamton Symposium in Geomorphology*, Rhoads BL, Thorn CE (eds). John Wiley and Sons: Chichester, U.K.; 147-170.

Demarchi L, Bizzi S, Piégay H. 2016. Regional hydromorphological characterization with continuous and automated remote sensing analysis based on VHR imagery and low-resolution LiDAR data. Earth Surface Processes and Landforms. DOI: 10.1002/esp.4092

Demarchi L, Bizzi S, Piégay H. 2017. Regional hydromorphological characterization with continuous and automated remote sensing analysis based on VHR imagery and low-resolution LiDAR data. Earth Surface Processes and Landforms **42**: 531-551. DOI: doi:10.1002/esp.4092

Eaton B, Millar R. 2017. Predicting gravel bed river response to environmental change: the strengths and limitations of a regime-based approach. Earth Surface Processes and Landforms **42**: 994-1008. DOI: doi:10.1002/esp.4058

Fausch KD, Torgersen CE, Baxter CV, Li HW. 2002. Landscapes to riverscapes: Bridging the gap between research and conservation of stream fishes. Bioscience **52**: 483-498. DOI: 10.1641/0006-3568(2002)052[0483:ltrbtg]2.0.co;2

Fryirs K, Brierley GJ. 2010. Antecedent controls on river character and behaviour in partly confined valley settings: Upper Hunter catchment, NSW, Australia. Geomorphology **117**: 106-120. DOI: 10.1016/j.geomorph.2009.11.015

Fryirs KA, Brierley GJ. 2018. What's in a name? A naming convention for geomorphic river types using the River Styles Framework. PLoS One **13**: e0201909. DOI: 10.1371/journal.pone.0201909

Fryirs KA, Wheaton JM, Brierley GJ. 2016. An approach for measuring confinement and assessing the influence of valley setting on river forms and processes. Earth Surface Processes and Landforms **41**: 701-710. DOI: 10.1002/esp.3893

Gilbert JT, Macfarlane WW, Wheaton JM. 2016. The Valley Bottom Extraction Tool (V-BET): A GIS tool for delineating valley bottoms across entire drainage networks. Computers & Geosciences **97**: 1-14. DOI: 10.1016/j.cageo.2016.07.014

Hall JE, Holzer DM, Beechie TJ. 2007. Predicting River Floodplain and Lateral Channel Migration for Salmon Habitat Conservation1. JAWRA Journal of the American Water Resources Association **43**: 786-797. DOI: 10.1111/j.1752-1688.2007.00063.x

Holmgren P. 1994. Multiple flow direction algorithms for runoff modelling in grid based elevation models: An empirical evaluation. Hydrological Processes **8**: 327-334. DOI: 10.1002/hyp.3360080405

Kellerhals R, Church M, Bray DI. 1976. Classification and Analysis of River Processes. Journal of the Hydraulics Division-Asce **102**: 813-829

Lindsay JB. 2016. Whitebox GAT: A case study in geomorphometric analysis. Computers & Geosciences **95**: 75-84. DOI: http://dx.doi.org/10.1016/j.cageo.2016.07.003

Lisenby PE, Fryirs KA. 2017. 'Out with the Old?' Why coarse spatial datasets are still useful for catchment-scale investigations of sediment (dis)connectivity. Earth Surface Processes and Landforms **42**: 1588-1596. DOI: 10.1002/esp.4131

Macfarlane WW, Wheaton JM, Bouwes N, Jensen ML, Gilbert JT, Hough-Snee N, Shivik JA. 2015. Modeling the capacity of riverscapes to support beaver dams. Geomorphology. DOI: 10.1016/j.geomorph.2015.11.019

McKay L, Bondeild T, Dewald T, Rea A, Johnston C, Moore R. 2012. NHDPlus Version 2: User Guide. U.S. Environmental Protection Agency.

Montgomery D, Buffington J. 1998. Channel processes, classification, and response. In *River Ecology and Management*, Naiman R, Bilbly RE (eds). Springer-Verlag: New York; 13-42.

Nagel DE, Buffington JM, Parkes SL, Wenger S, Goode JR. 2014. A landscape scale valley confinement algorithm: Delineating unconfined valley bottoms for geomorphic, aquatic, and riparian applications. In *General Technical Report (GTR)*. U.S. Department of Agriculture, Forest Service, Rocky Mountain Research Station: Fort Collins, CO; 42.

Notebaert B, Piegay H. 2013. Multi-scale factors controlling the pattern of floodplain width at a network scale: The case of the Rhone basin, France. Geomorphology **200**: 155-171. DOI: 10.1016/j.geomorph.2013.03.014

O'Brien G, Wheaton JM. 2015. River Styles Report for the Middle Fork John Day Watershed, Oregon - Example Report for Exploring Leveraging the River Styles Framework in Tributary Habitat Management for the Columbia River Basin. Ecogeomorphology and Topographic Analysis Lab, Utah State University, Prepared for Eco Logical Research and the Bonneville Power Administration: Logan, UT; 207.

O'Brien GR, Stevens G, Macfarlane WW, Wheaton JM. 2019. Geomorphic Assessment of the White River--valley landform delineation, reach typing, and geomorphic condition. Utah State University Ecogeomorphology and Topographic Analysis Lab: Logan, UT; 86.

O'Brien GR, Wheaton J, Fryirs K, McHugh P, Bouwes N, Brierley G, Jordan C. 2017. A geomorphic assessment to inform strategic stream restoration planning in the Middle Fork John Day Watershed, Oregon, USA. Journal of Maps **13**: 369-381. DOI: 10.1080/17445647.2017.1313787

Omernik JM, Griffith GE. 2014. Ecoregions of the Conterminous United States: Evolution of a Hierarchical Spatial Framework. Environmental Management **54**: 1249-1266. DOI: 10.1007/s00267-014-0364-1

Passalacqua P, Belmont P, Staley D, Simley J, Arrowsmith JR, Bodee C, Crosby C, DeLong SB, Glenn NF, Kelly S, Lague D, Sangireddy H, Schaffrath K, Tarboton D, Wasklewicz T, Wheaton J. 2015. Analyzing high resolution topography for advancing the understanding of mass and energy transfer through landscapes: A review. Earth Science Reviews **148**: 174-193. DOI: 10.1016/j.earscirev.2015.05.012

Reinfelds I, Cohen T, Batten P, Brierley G. 2004. Assessment of downstream trends in channel gradient, total and specific stream power: a GIS approach. Geomorphology **60**: 403-416. DOI: 10.1016/j.geomorph.2003.10.003

Rosgen D. 1996. Applied River Morphology. Wildland Hydrology: Pagosa Springs, CO

Rosgen DL. 1994. A Classification of Natural Rivers. Catena **22**: 169-199

Roux C, Alber A, Bertrand M, Vaudor L, Piégay H. 2014. "FluvialCorridor": A new ArcGIS toolbox package for multiscale riverscape exploration. Geomorphology. DOI: 10.1016/j.geomorph.2014.04.018

Roux C, Alber A, Bertrand M, Vaudor L, Piégay H. 2015. "FluvialCorridor": A new ArcGIS toolbox package for multiscale riverscape exploration. Geomorphology **242**: 29-37. DOI: https://doi.org/10.1016/j.geomorph.2014.04.018

Schaffrath KR, Belmont P, Wheaton JM. 2015. Landscape-scale geomorphic change detection: Quantifying spatially variable uncertainty and circumventing legacy data issues. Geomorphology **250**: 334-348. DOI: 10.1016/j.geomorph.2015.09.020

Sciences W. 2010. LiDAR Remote Sensing Data Collection: Tucannon River, Tucannon Headwaters, and Cummins Creek, WA. Watershed Sciences: Portland, OR; 35.

Stout JC, Belmont P. 2013. TerEx Toolbox for semi-automated selection of fluvial terrace and floodplain features from lidar. Earth Surface Processes and Landforms: n/a-n/a. DOI: 10.1002/esp.3464

Stout JC, Belmont P. 2014. TerEx Toolbox for semi-automated selection of fluvial terrace and floodplain features from lidar. Earth Surface Processes and Landforms **39**: 569-580. DOI: 10.1002/esp.3464

Thorson TD, Bryce SA, Lammers DA, Woods AJ, Omernik JM, Kagan J, Pater DE, Comstock JA. 2003. Ecoregions of Oregon (color poster with map, descriptive text, summary tables, and photographs). U.S. Geological Survey: Reston, Virginia,.

Tinkler KJ, Wohl EE. 1998. A Primer on Bedrock Channels. In *Rivers over Rock*, Tinkler KJ, Wohl EE (eds). American Geophysical Union; 1-18.

USGS. 1999. National Elevation Dataset. U.S. Geological Survey; 2.

USGS. 2007. National Hydrography Dataset. United States Geological Survey (USGS); The National Hydrography Dataset (NHD) is the surface water component of The National Map. The NHD is a digital vector dataset used by geographic information systems (GIS). It contains features such as lakes, ponds, streams, rivers, canals, dams and streamgages. These data are designed to be used in general mapping and in the analysis of surface-water systems.

Wheaton J, Fryirs K, Brierley GJ, Bangen SG, Bouwes N, O'Brien G. 2015. Geomorphic Mapping and Taxonomy of Fluvial Landforms. Geomorphology **248**: 273-295. DOI: 10.1016/j.geomorph.2015.07.010

Williams BS, D'Amico E, Kastens JH, Thorp JH, Flotemersch JE, Thoms MC. 2013. Automated riverine landscape characterization: GIS-based tools for watershed-scale research, assessment, and management. Environmental Monitoring and Assessment **185**: 7485-7499. DOI: 10.1007/s10661-013-3114-6

Wohl E. 2013. Channel Morphology. In *Mountain Rivers Revisited*. American Geophysical Union; 229-257.

Wohl E, Dwire K, Sutfin N, Polvi L, Bazan R. 2012. Mechanisms of carbon storage in mountainous headwater rivers. **3**: 1263. DOI: 10.1038/ncomms2274

Wolman MG, Miller JP. 1960. Magnitude and frequency of forces in geomorphic processes. Journal of Geology **68**: 54-74

Table 1 - Examples of freely available datasets with nationwide coverage that could be used to derive valley bottom margin input (e.g. DEMs) and channel margin inputs (e.g. drainage network) from which confinement can be calculated. List is non-exhaustive.

Country	Digital Elevation Models (DEMs)	Drainage Network
Australia	National Elevation Data Framework (NEDF) 5 m resolution DEM: http://www.ga.gov.au/scientific-topics/national-location-information/digital-elevation-data#heading-2	The National Surface Hydrology Database: http://www.ga.gov.au/scientific-topics/national-location-information/national-surface-water-information
Canada	The Canadian Digital Elevation Model (CDEM) 0.75 arc seconds resolution DEM (c. 22 m)* : http://maps.canada.ca/czs/index-en.html	Canadian National Hydro Network (NHN): http://maps.canada.ca/czs/index-en.html
New Zealand	Land Information New Zealand (LINZ) 8 m resolution DEM: https://data.linz.govt.nz/layer/51768-nz-8m-digital-elevation-model-2012/	Land Information New Zealand (LINZ) Hydrographic Data: https://www.linz.govt.nz/data/linz-data/hydrographic-data
Spain	Spanish National Geographic Institute : 5 m resolution DEM; http://contenido.ign.es/csw-inspire/srv/spa/main.home?uuid=spaignMDT05201307180727	
United Kingdom	Ordnance Survey (OS), Great Britain OS Terrain 5 DTM: https://data.gov.uk/dataset/os-terrain-5-dtm	United Kingdom Hydrographic Office (UKHO)
United States of America	National Elevation Dataset (NED) 10 m resolution DEM: https://nationalmap.gov/elevation.html	National Hydrologic Datastet (NHD) 1:24K Cartographic Network (cartographic is desirable to NHD+ hydrographic): https://nhd.usgs.gov/

Table 2. Measures of valley margin and valley bottom confinement used to discriminate valley settings and first order river types (modified from Fryirs et al., 2016). Note: this does not cover all river types or all possible combinations within ranges. See Fryirs and Brierley (2018) for examples of these river types and names.

Valley setting (river type)	Valley margin confinement (C_V)	Valley bottom confinement (C_{VB})	Dominant confining medium
Confined rivers			
Confined (e.g. bedrock margin-controlled, gorge, boulder bed)	C_V =100%	C_{VB} = 100%	Bedrock
Confined (e.g. bedrock margin-controlled, occasional floodplain pockets, boulder bed)	$C_V \geq 85\%$	$C_{VB} \geq 85\%$	Bedrock
Confined valley (terrace margin-controlled, cobble bed)	$C_V \leq 10\%$	$C_{VB} \geq 85\%$	Terrace
Partly confined, margin-controlled rivers			
Partly confined (e.g. bedrock margin-controlled, discontinuous floodplain, gravel bed)	C_V = 50-85%	$C_{VB} \geq$ 50-85%	Bedrock
Partly confined (e.g. fan margin-controlled, discontinuous floodplain, gravel bed)	C_V = 50-85%	$C_{VB} \geq$ 50-85%	Fan
Partly confined, planform-controlled rivers			
Partly confined (e.g. planform-controlled, low sinuosity, discontinuous floodplain, gravel bed)	C_V = 10-50%	C_{VB} =10-50%	Bedrock
Partly confined (e.g. planform-controlled, low sinuosity, fan constrained, discontinuous floodplain, gravel bed)	C_V = 10-50%	C_{VB} = 10-50%	Fan
Laterally unconfined rivers			
Laterally unconfined (e.g. continuous channel, meandering, sand bed)	$C_V \leq 10\%$	$C_{VB} \leq 10\%$	None
Laterally unconfined (e.g. discontinuous channel, valley fill, fine grained)	C_V = 0% (no channel)	C_{VB} = 0% (no channel)	
Anthropogenically controlled or constrained rivers			
Confined or partly confined (e.g. stopbank margin-controlled, or	Any range ($C_A > C_V$) Where C_A =	Any range ($C_A > C_{VB}$) Where C_A =	

constrained)	anthropogenic margin	anthropogenic margin	

Table 3. Primary physiographic attributes of study watersheds. See Figure 4 for ecoregions.

Watershed	Area *(km^2)*	Length of Perennial Streams *(km)*	Relief *(m)*	Dominant Lithologies	Ecoregions
Middle Fork John Day, Oregon	2052	4110	1615	Tertiary volcanics, Columbia River Basalt group, metasedimentary marine rocks	Uplands, highlands, mélange, mesic forests, subalpine-alpine
Grand Ronde, Oregon	4238	3402	1933	Tertiary volcanics, Columbia River Basalt group.	Maritime, mountainous, canyons and dissected highlands, continental foothills, mountain basins, mesic forests, subalpine-alpine
Tucannon, Washington	1302	1108	1778	Tertiary volcanics, Columbia River Basalt group	Loess, dissected loess uplands, deep loess foothills, maritime, canyons and dissected highlands, mesic forests
Upper Salmon, Idaho	928	731	1396	Dominantly granitics, with smaller regions of sedimentary (limestone and sandstone) and volcanic rocks	Uplands, high glacial drift valleys, batholith, forested mountains
TOTAL	8520	9351	NA	NA	NA

Table 4. Percent stream length reported in valley bottom confinement categories using EMC, and modeled techniques in the Upper Salmon watershed. *Note:* both manual and modeled outputs were analyzed on the same perennial network extent segmented at 500 m.

Analysis	Total stream length (km)	Valley setting (% total stream length)			
		Laterally unconfined	Partly confined, planform-controlled	Partly confined, margin-controlled	Confined
Manual (EMC)	729	42% (306 km)	9% (66 km)	19% (139 km)	30% (219 km)
Modeled	729	31% (226 km)	19% (139 km)	22% (160 km)	28% (204 km)
Difference	0	-11% (80 km)	+10% (73 km)	+3% (22 km)	-2% (15 km)
			Lumped (all partly confined)		
Manual (EMC)	729	42% (306 km)	28% (205 km)		30% (219 km)
Modeled	729	31% (226 km)	41% (299 km)		28% (204 km)
Difference	0	-11% (80 km)	+13% (95 km)		-2% (15 km)

Table 5. Impact of basemap resolution on confinement values (summarized into categories) calculated for the mainstem Tucannon River using 1-m and 10-m DEMs, both datasets were segmented at 500 m. Percent differences reflect the degree to which the coarser 10 m DEMs over-predict a class where positive, and under-predict where negative.

Base DEM resolution	Total stream length (km)	Valley Setting Categories (% total stream length)			
		Laterally unconfined	Partly confined, planform-controlled	Partly confined, margin-controlled	Confined
1-m LiDAR	156	50% (78km)	28% (44 km)	14% (22 km)	8% (12 km)
10-m NED	118	33% (39 km)	35% (41 km)	18% (21 km)	14% (17 km)
Difference	-38	-17% (-39 km)	+7% (3 km)	+4% (1 km)	+6% (5 km)
		Laterally unconfined	Partly confined		Confined
1-m LiDAR	156	50% (78km)	42% (66 km)		8% (12 km)
10-m NED	118	33% (39 km)	53% (62 km)		14% (17 km)
Difference	-38	-17% (-39 km)	+11% (3 km)		+6% (5 km)

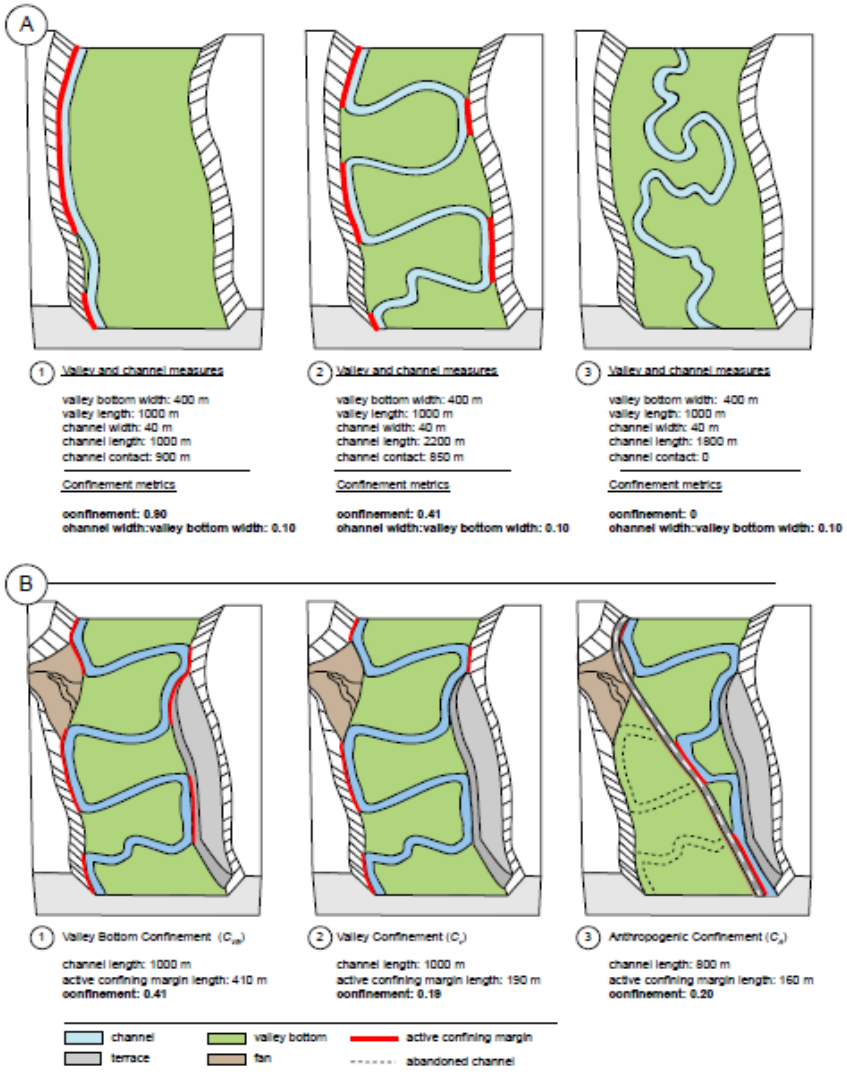

Figure 1. (A) Comparison of confinement calculated as a ratio of channel width to valley bottom width (CW:VBW). Scenarios 1-3 have identical valley bottom dimensions and channel widths, but differing channel lengths and channel contact with active confining margins. Calculations result in a single value of CW:VBW but three measures of confinement that help differentiate confined, partly confined and laterally unconfined valley settings; (B) Examples of various types of confinement that can be calculated with prepared potential confinement margin polygons as inputs to the Confinement Tool: (1) valley bottom, (2) valley, and (3) anthropogenic confinement.

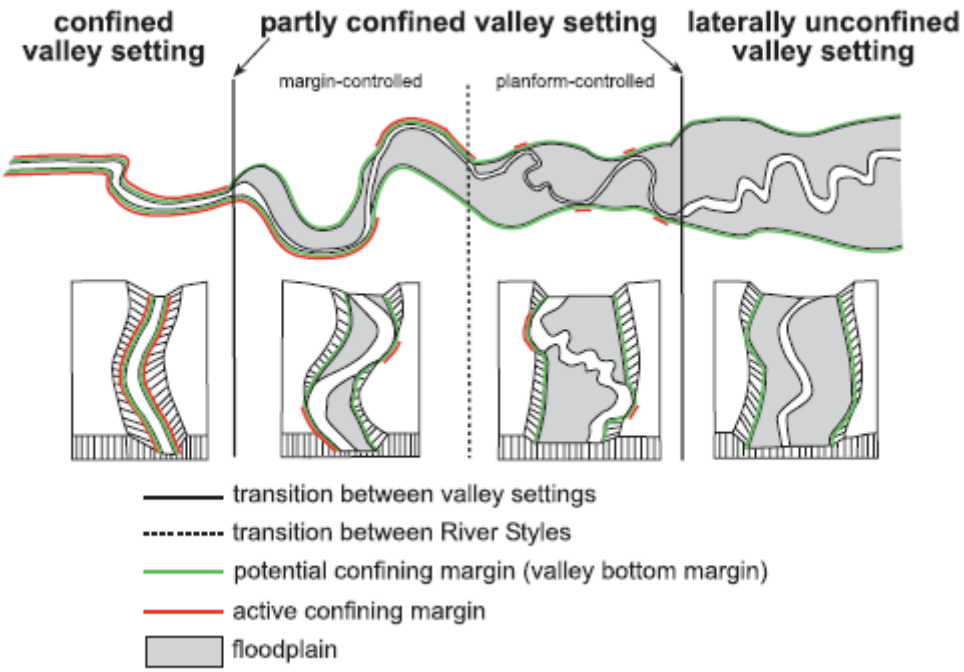

Figure 2. Illustration of transitions across contrasting valley settings along a continuum of valley bottom confinement. Decreasing contact between the channel and the valley bottom margin (from left to right) results in progressively less active confining margin (pink). Modified from Fryirs and Brierley (2010).

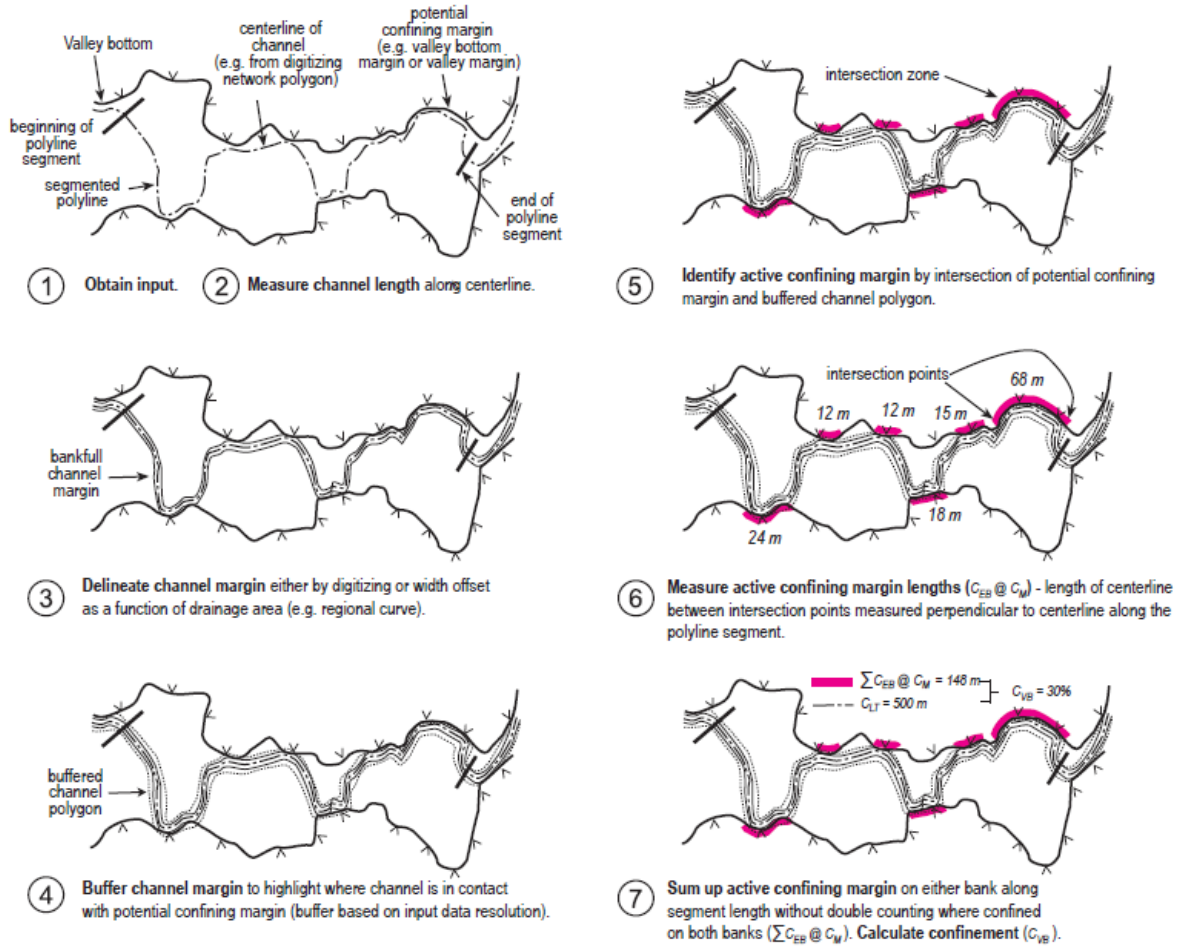

Figure 3. Illustration of workflow for confinement calculation for an individual drainage network segment.

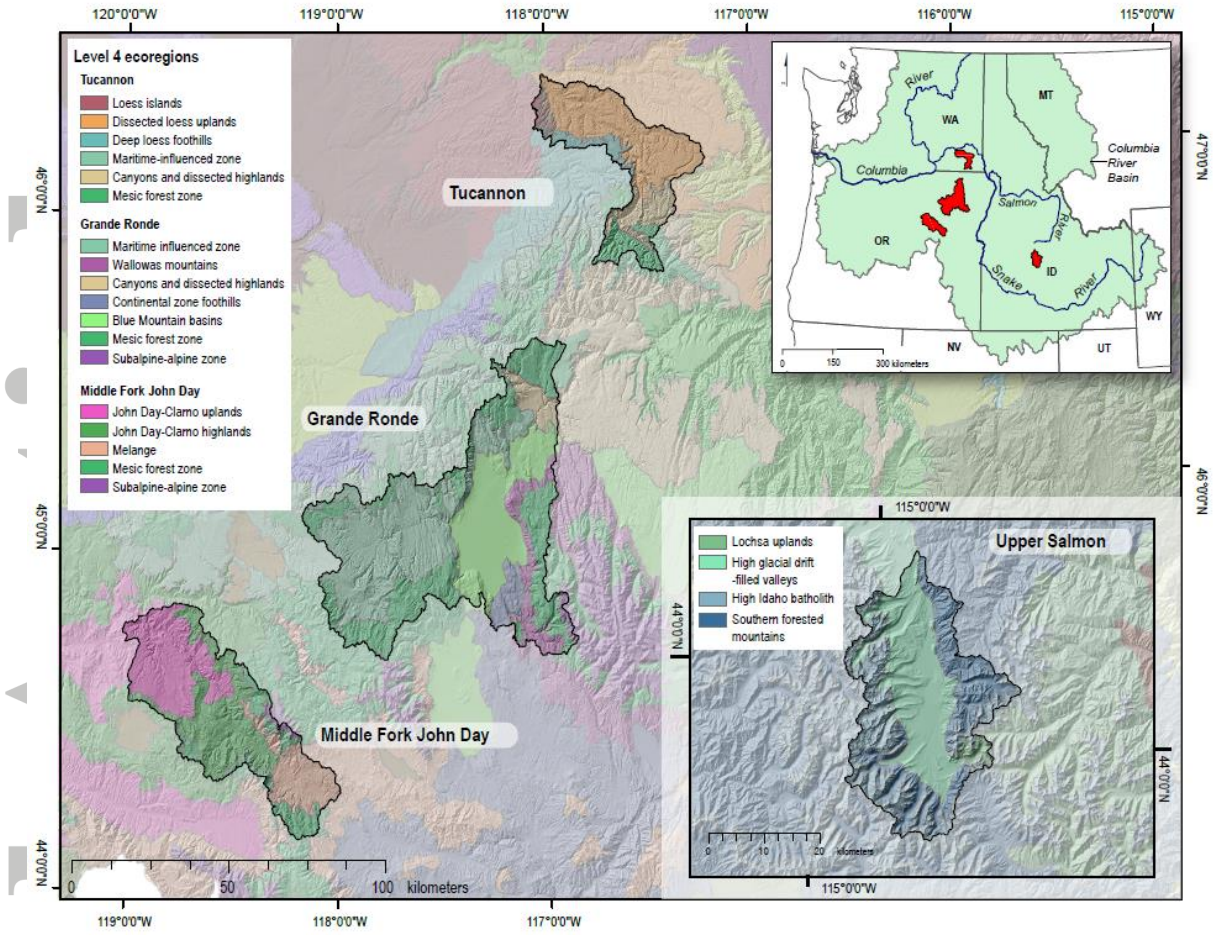

Figure 4. Location of four study watersheds within the interior Columbia River Basin in the Pacific Northwest United States. Underlying hillshade and Level 4 ecoregions (Omernik and Griffith, 2014; Thorson*, et al.*, 2003) illustrate the physiographic diversity of these four watersheds.

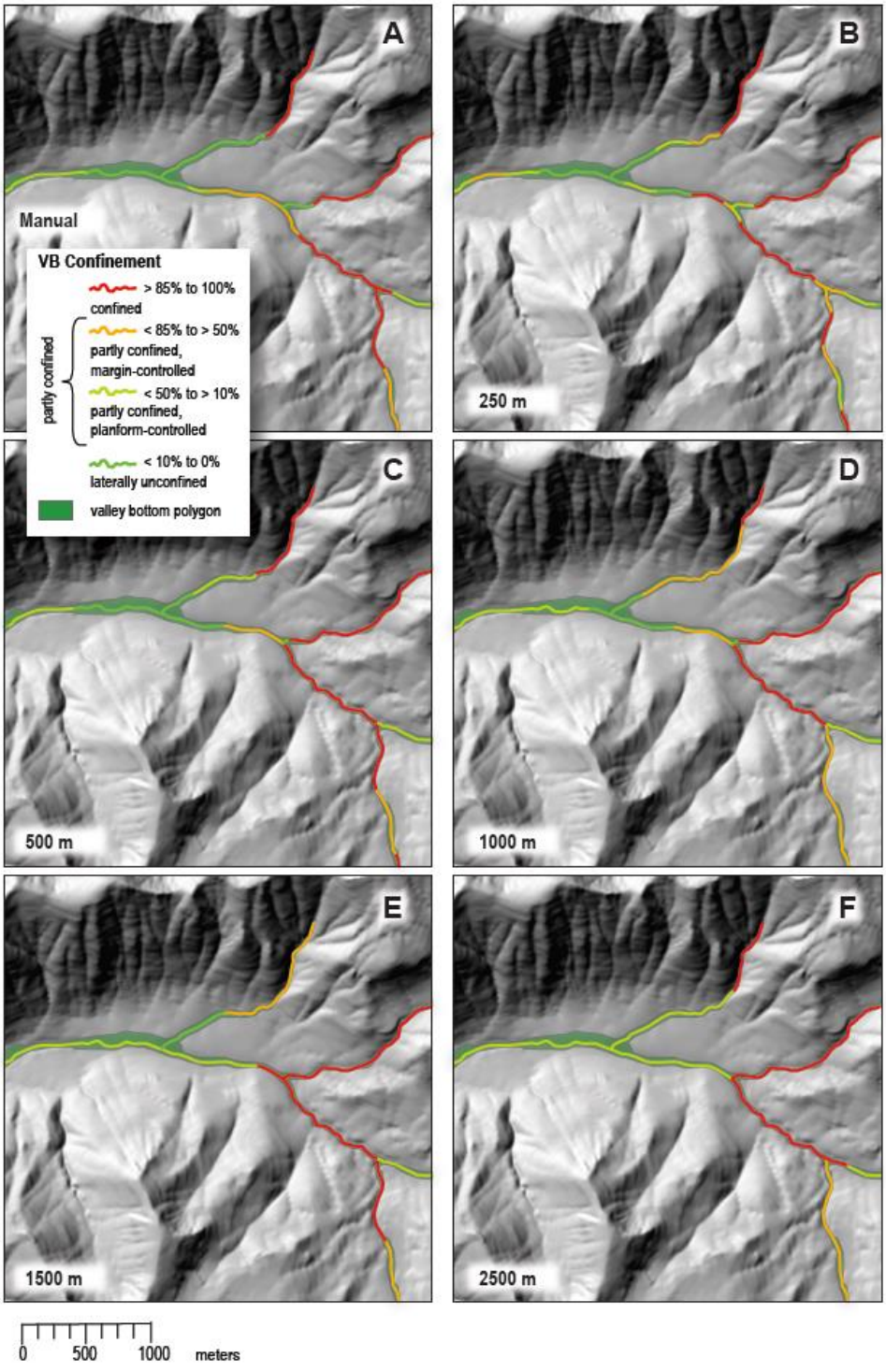

Figure 5. An example illustration from 4th of July Creek in the Upper Salmon watershed (Idaho, USA) showing the sensitivity of confinement calculations (illustrated categorically) relative to the length of network segmentation. When uniformly segmented, shorter segment lengths (i.e. CL_T) still exist between tributary junctions, but the uniform segmentation length (e.g. 250, 500, 1000, 1500 or 2500 m)

represents the maximum segment length. (A) Delineated confinement values with variable segmentation length based on manual segmentation at expert-identified reach breaks. (B – F) Contrasting confinement values when confinement is calculated with different maximum segment lengths (i.e.CL_T) specified.

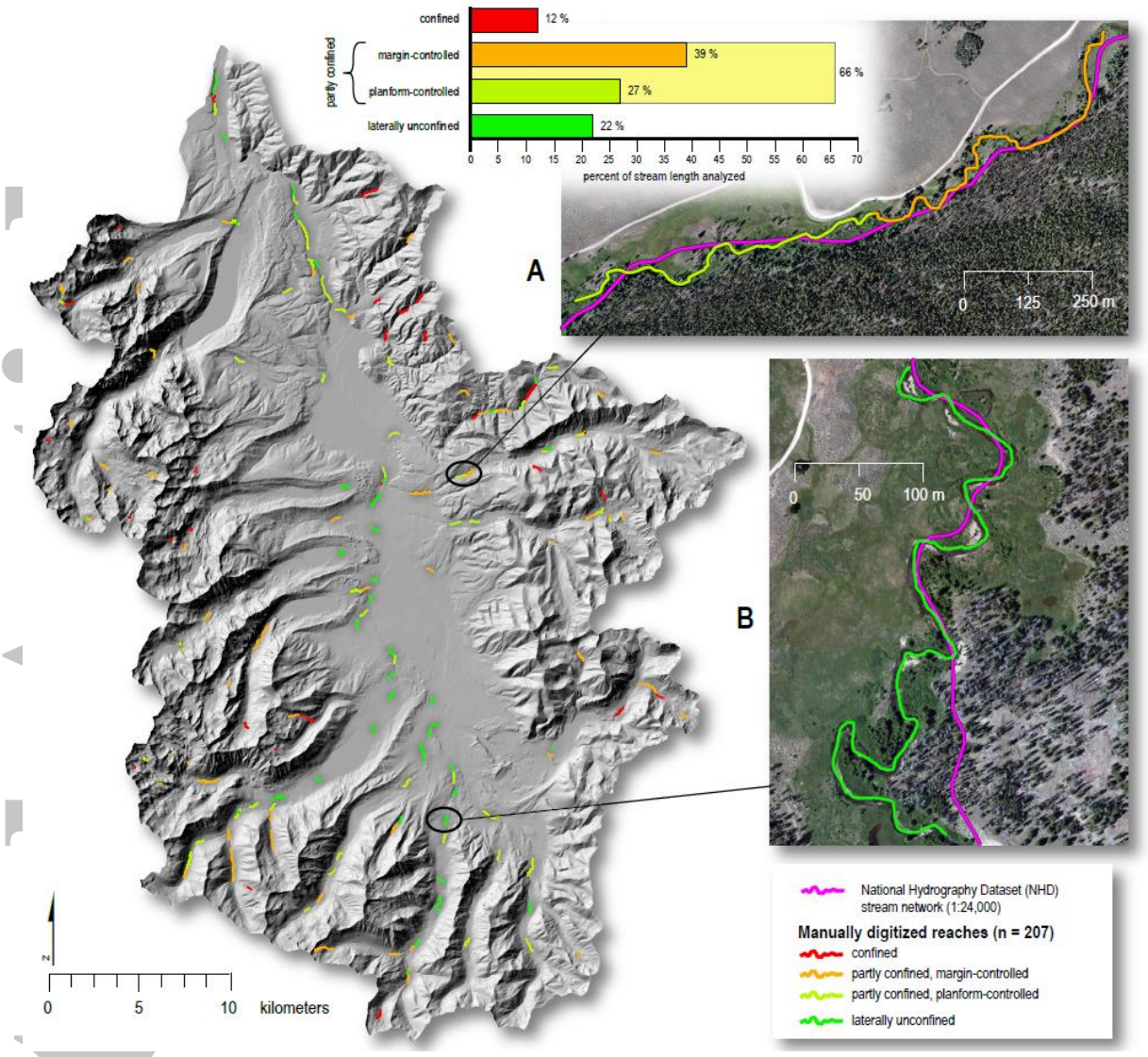

Figure 6. Distribution of randomly selected reaches comprising equal numbers (*n* ~50) of valley settings (laterally unconfined; partly confined, planform-controlled, partly confined; partly confined, margin-controlled; and confined) in the Upper Salmon watershed, Idaho. Bar plot shows percentages of each confinement category in the dataset (*n* = 207) when digitized streamlines are used as an input for the tool. Inset photographs show channel planforms depicted by NHD streamline and by manually measured and digitized techniques. (A) Partly confined reaches on 4th of July Creek; (B) Laterally unconfined valley in lower Smiley Creek.

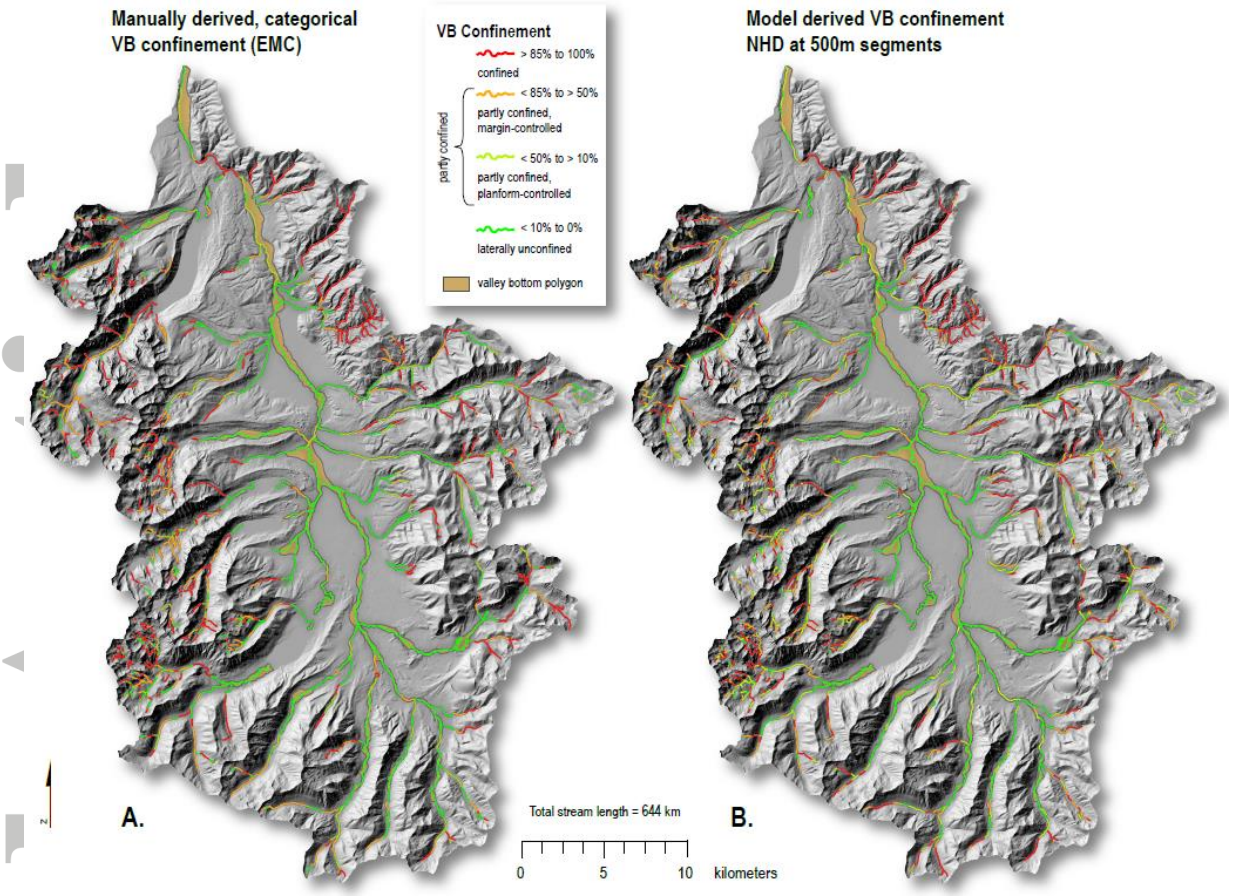

Figure 7. Comparison of valley bottom (VB) confinement calculated in the Upper Salmon watershed by (A) manually derived, categorical VB confinement (EMC); and (B) modeled using the Confinement Tool. Both use an NHD stream network segmented at 500 m lengths.

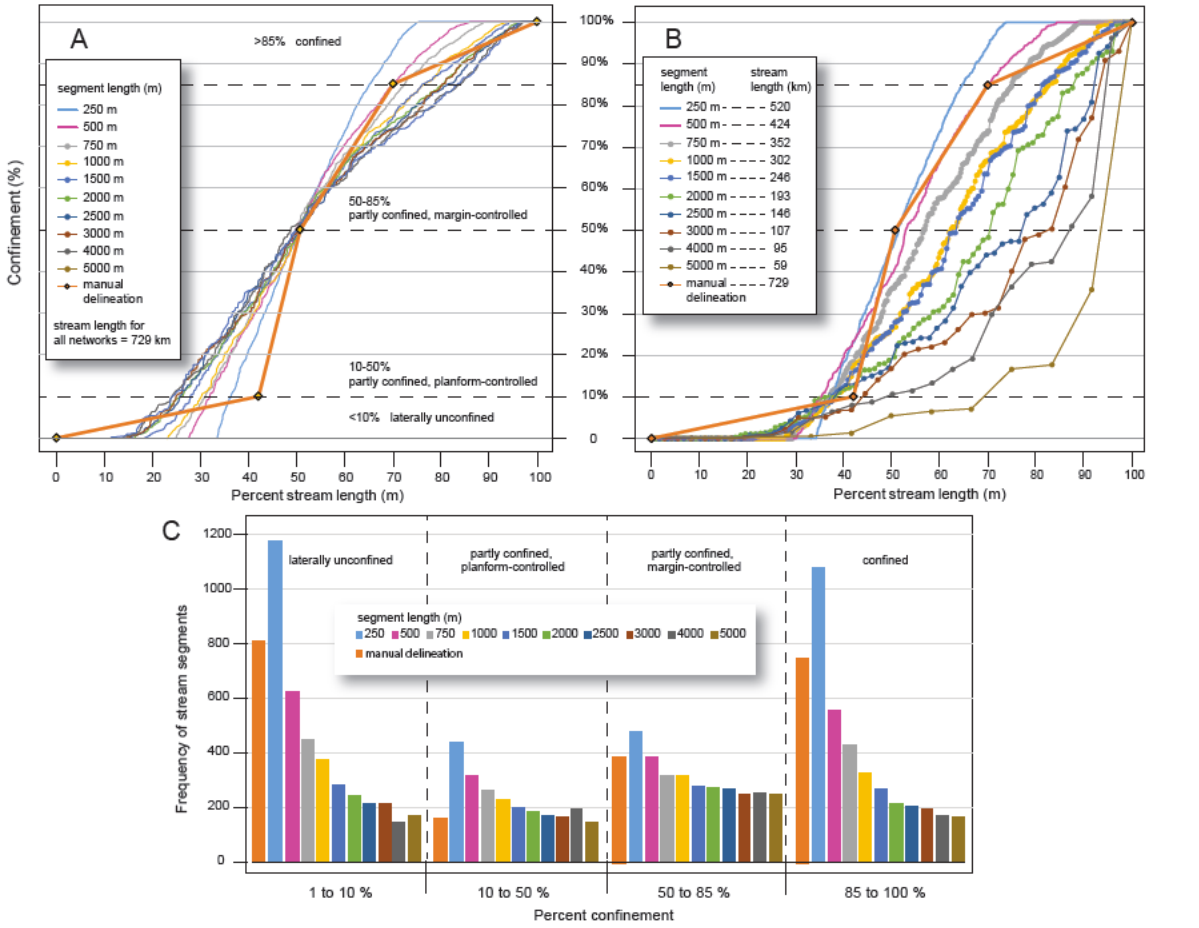

Figure 8. Categorical EMC and modeled confinement in the Upper Salmon watershed, showing the entire network segmented at each interval (stated segment length plus all shorter lengths forced by node-to-node NHD structure). A and B are percent stream length vs confinement per NHD network segmented at various lengths; C is frequency of total segments that fall within the broad confinement ranges, for various intervals.

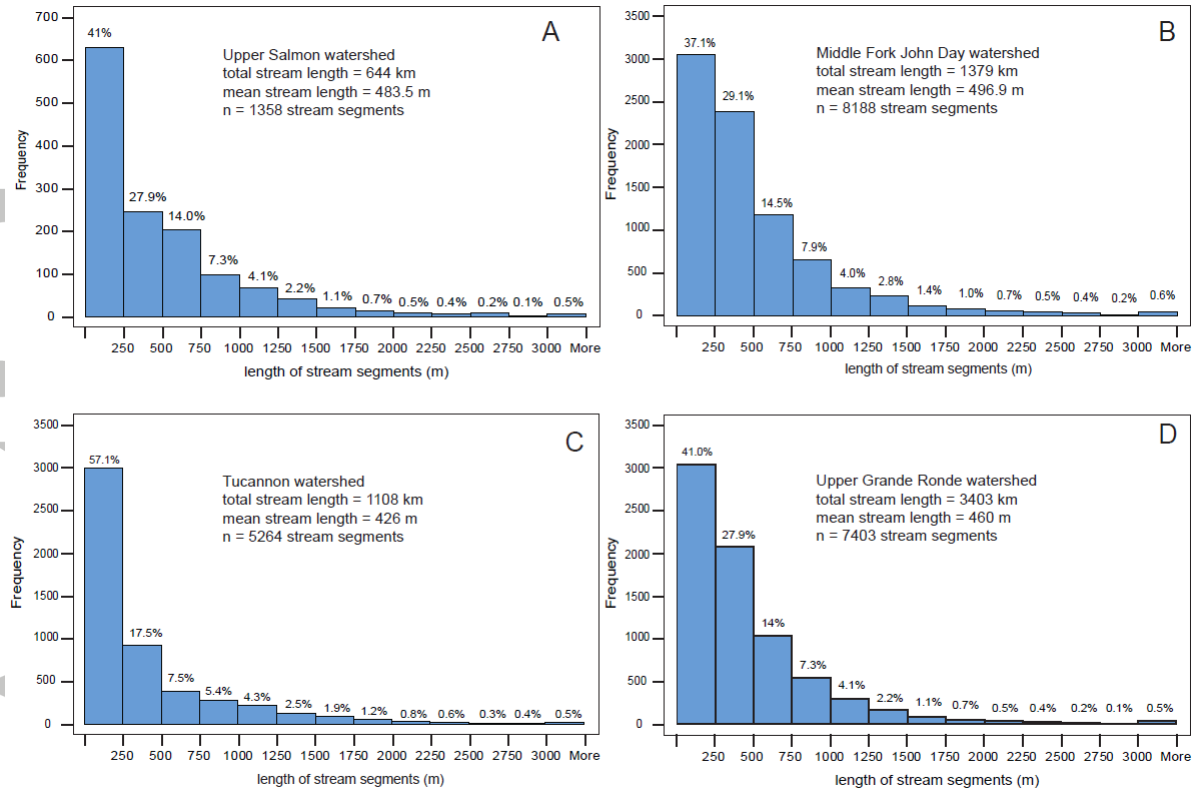

Figure 9. Frequency distribution and percentage of segment lengths from NHD drainage networks in the four study watersheds. (A) Upper Salmon; (B) Middle Fork John Day; (C) Tucannon; and (D) Upper Grande Ronde.

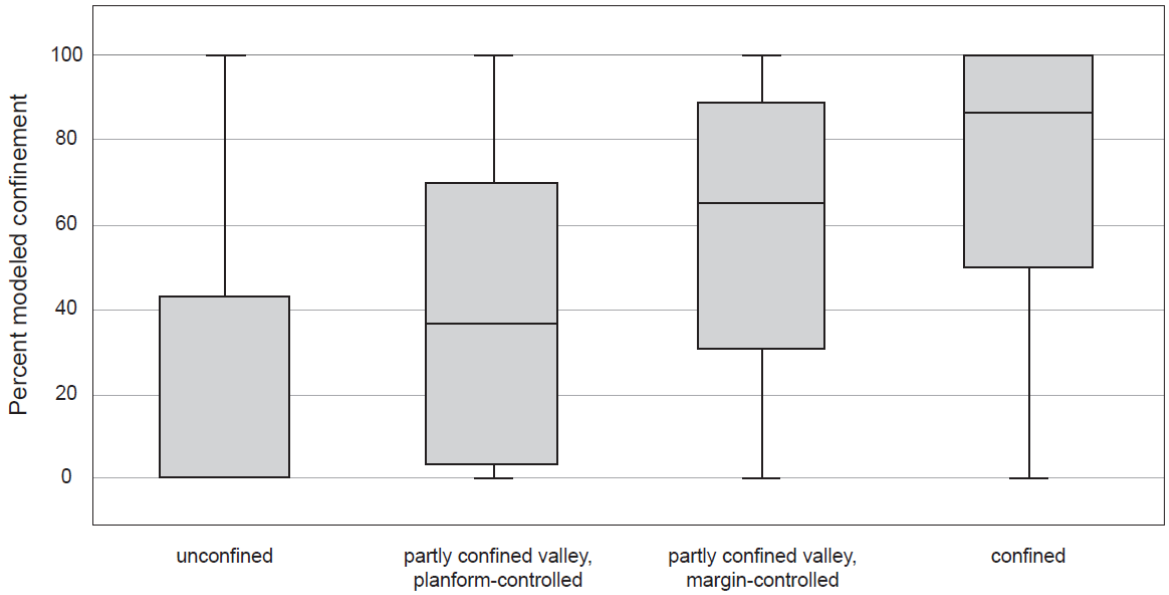

Figure 10. Box plot for Upper Salmon watershed, showing distribution of modeled confinement values (i.e. Figure 8B segmented at 500 m) broken out by manually classified valley settings (i.e. Figure 8A).

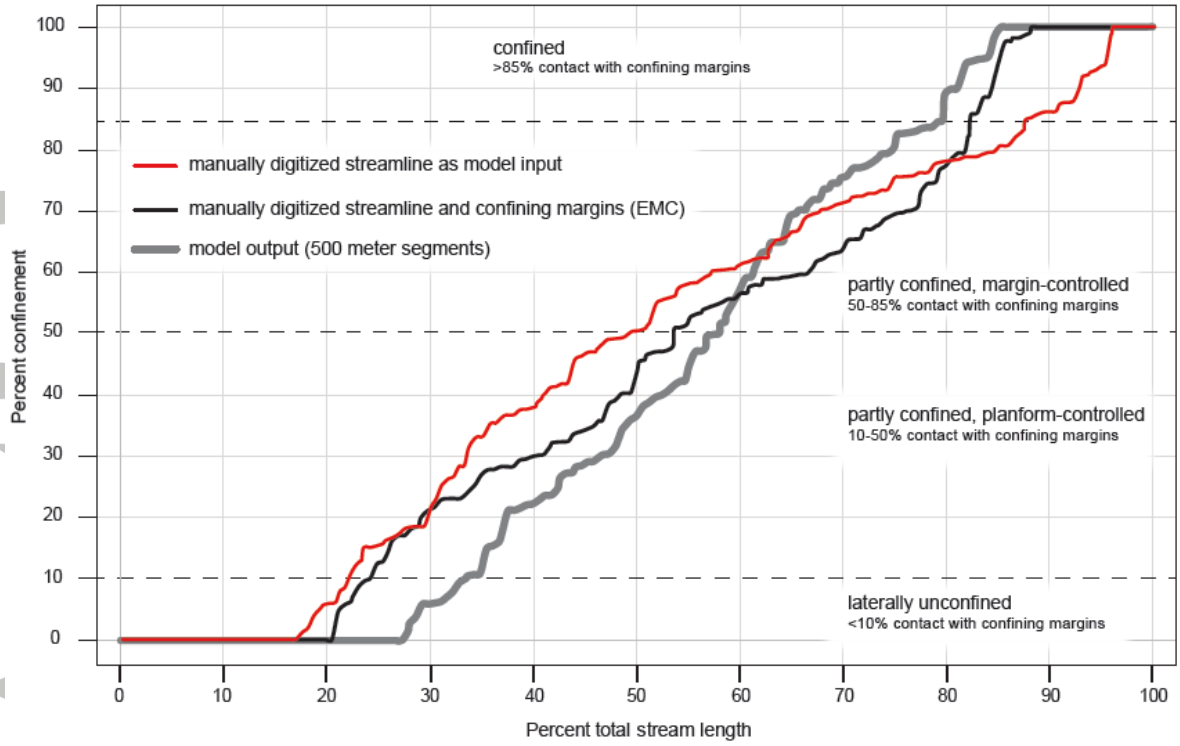

Figure 11. Percent confinement versus total stream length for 207 randomly selected reaches in the Upper Salmon watershed. Confinement estimates are contrasted for (a) manually digitized planforms and confining margins (EMC) (black); (b) digitized planforms used as model input (red), and (c) standard model output with stream reaches segmented at 500 m (grey).

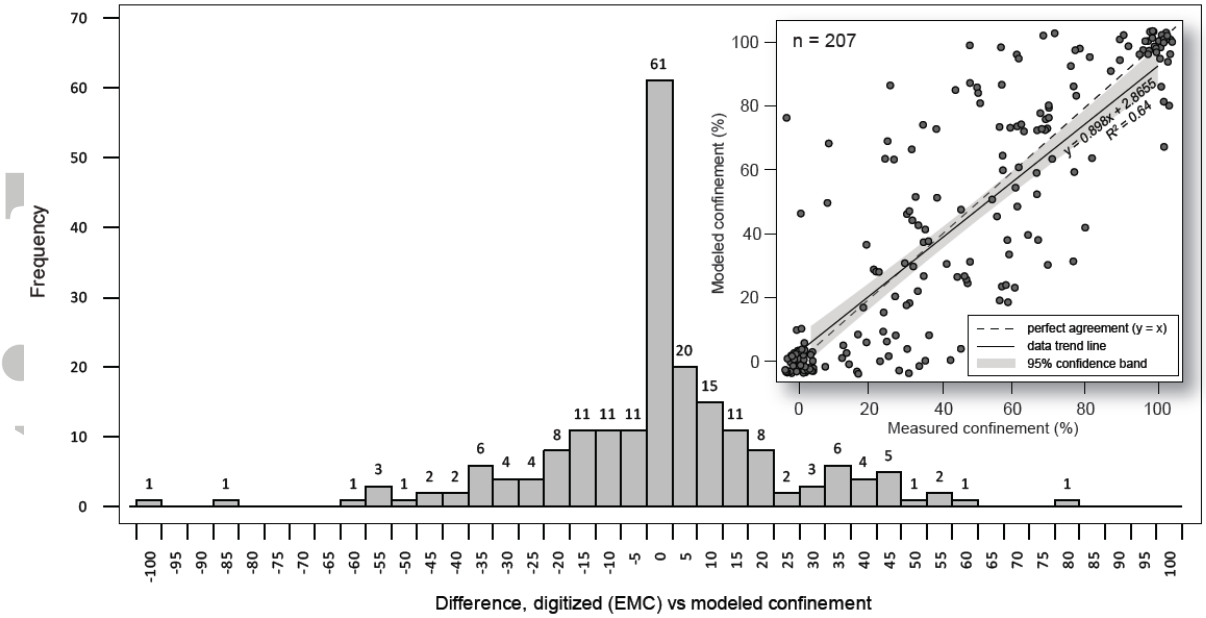

Figure 12. Distribution of difference between manually digitized planform and confining margins (EMC) and modeled confinement (500 m segments). Inset shows regression of values using “jitter plot” output where end-member unconfined (“0%”) and confined (“100%”) data are shown tightly clustered rather than stacked to ensure that confinement values equal to 0 and 1 are discernible from a single point at each end.

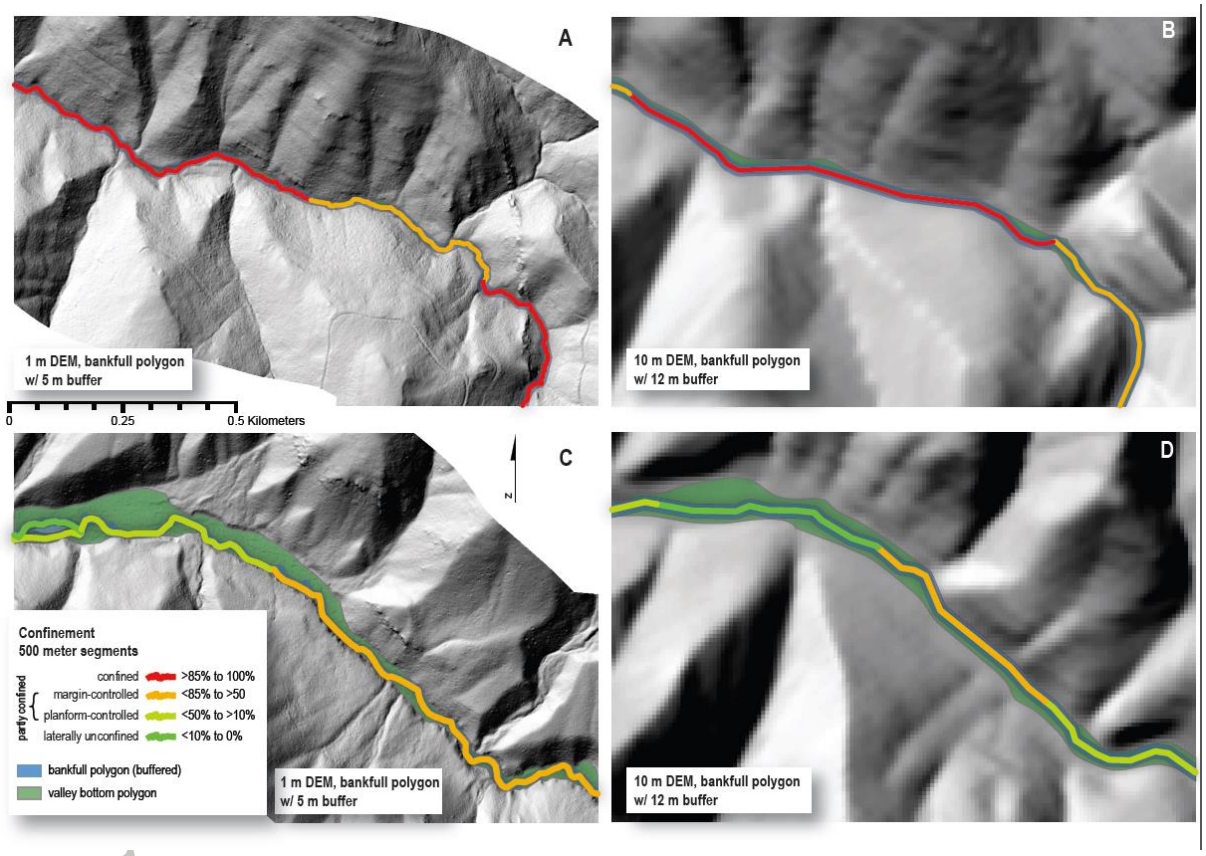

Figure 13. Confinement calculated using LiDAR versus 10m DEM in a confined valley setting (A and B, respectively), and in a partly confined valley setting (C and D, respectively).

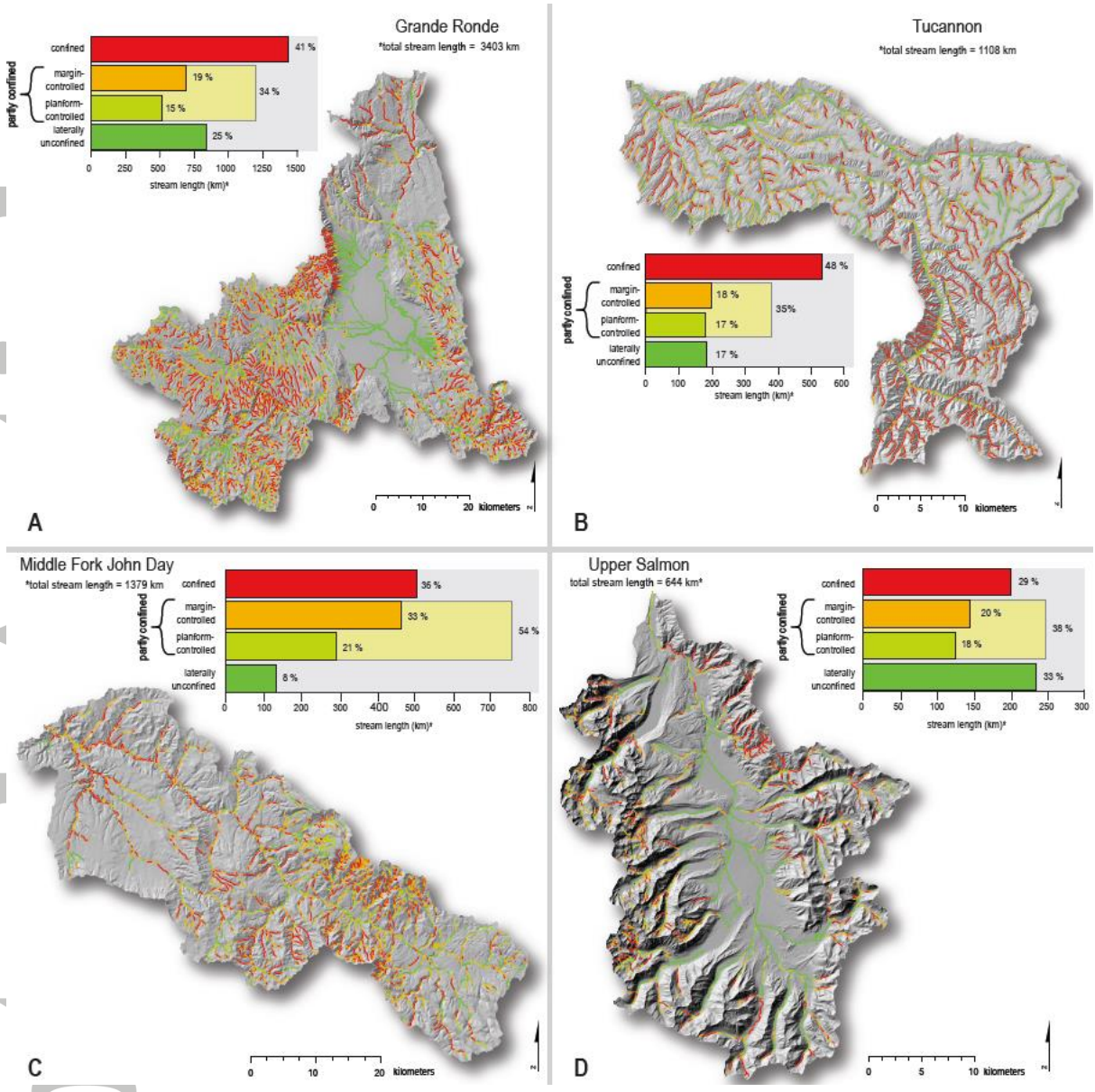

Figure 14. Basin-wide confinement for the four study watersheds of the interior Columbia River Basin (A) Grande Ronde; (B) Tucannon; (C) Middle Fork John Day and (D) Upper Salmon. Bar plots show percentage of confinement in each valley setting.

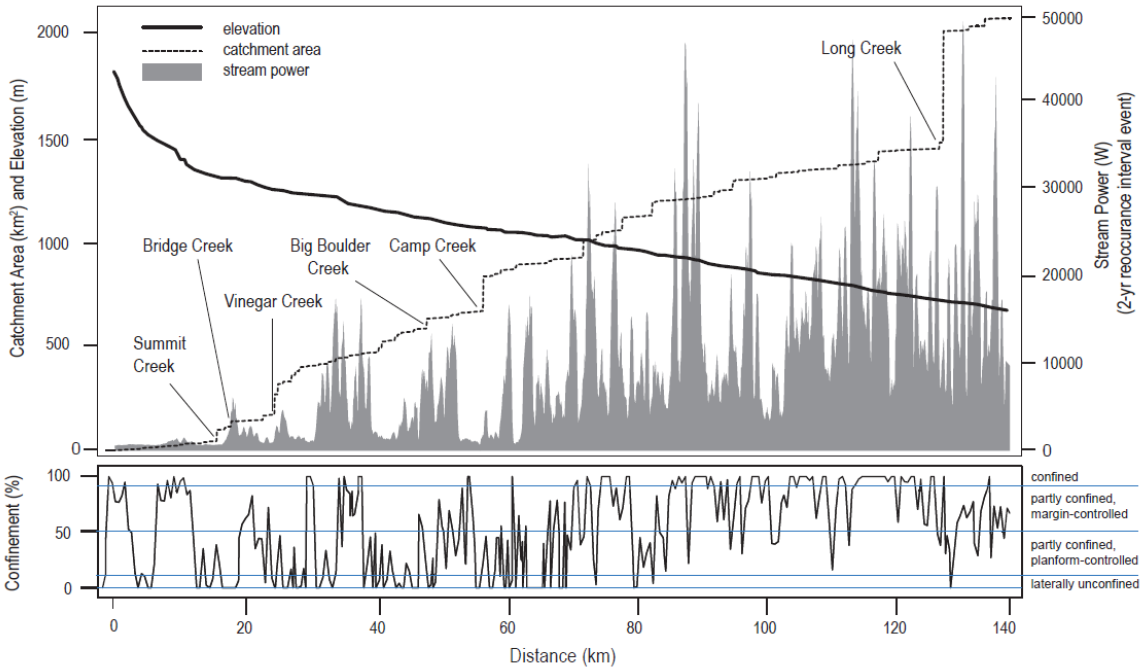

Figure 15. Example of a stacked-profile plot for the mainstem of Middle Fork John Day River showing downstream relationship between valley bottom confinement (bottom) and conventional approaches to analysis of controls upon patterns of river morphodynamics (gross stream power, longitudinal profile, and drainage area).